CHAPTER 12

Topological Theory of Defects

In Chapter 3, we have considered the notion of order parameter, its amplitude and phase. The order parameter is a continuous field (scalar, vector, tensor, etc.) describing the state of the system at each point. Generally, it is a function of coordinates, $\psi(\mathbf{r})$. Distortions of $\psi(\mathbf{r})$ can be of two types: those containing singularities and those without singularities. At singularities, ψ is not defined. For a 3D medium, the singular regions might be either zero-dimensional (points), one-dimensional (lines), or two-dimensional (walls). These are the *defects*. Whenever a nonhomogeneous state cannot be eliminated by continuous variations of the order parameter (i.e., one cannot arrive at the homogeneous state), it is called *topologically stable*, or simply, a *topological defect*. If the inhomogeneous state does not contain singularities, but nevertheless is not deformable continuously into a homogeneous state, one says that the system contains a *topological configuration* (or soliton).

Very often the problems involving defects are too complex for analytical treatment within the framework of an elastic theory. The difficulties arise either from the complexity of the free energy functional (biaxial nematic, smectic C, anisotropic phases of superfluid 3He, etc.) or from the complexity of the defect configuration (e.g., crossing of disclinations). Even when the solutions are possible, they rely on certain assumptions and, thus, might be strongly model dependent.

An adequate description of defects in ordered condensed media requires introducing a new mathematical apparatus, viz. the theory of homotopy, which is part of algebraic topology. It is precisely in the language of topology that it is possible to associate the character of ordering of a medium and the types of defects arising in it, to find the laws of decay, merger and crossing of defects, to trace out their behavior during phase transitions, and so on. The key point is occupied by the concept of *topological invariant*, often also called a *topological charge*, which is inherent in every defect. The stability of the defect is guaranteed by the conservation of its topological invariant. The following simple example of twisted ribbon strips gives a flavor of the concept of topological invariant.

12.1. Basic Concepts of Topological Classification

12.1.1. Topological Charges Illustrated with Möbius Strips

Consider a set of elastic strips closed into rings. Each strip is characterized by a number k that counts how many times the ends of the strip are twisted by 2π before they are glued together to produce a ring (Fig. 12.1). The ring with $k = 1/2$ (Fig. 12.1.b) is the well-known Möbius strip. The deformation energy stored in any twisted strip is larger than the pure bend energy of the $k = 0$ ring. However, to transform a twisted strip into a state $k = 0$, one needs to cut the strip. There is no continuous deformation that transforms one strip into another if the two have different k. The energy needed to cut the ribbon, $F_{\text{cut}} \sim US/a^2$, is much higher than the stored twist energy $F_{\text{twist}} \sim k^2 KS/L$; here, L is the length of the strip, S is its cross-section area, and $K \sim U/a$ is some elastic constant of the order of the intermolecular energy; a is the molecular scale. The transitions between the states with different k's are prohibited by high-energy barriers.

The quantity k does not change under any continuous transformation and is a useful invariant to label topologically different states. Left and right twists can be distinguished by the sign of k. Obviously, one can create a pair of left and right twists without cutting the strip, what matters is the total sum of k's that should be preserved. Therefore, topological charges k's obey a conservation law.

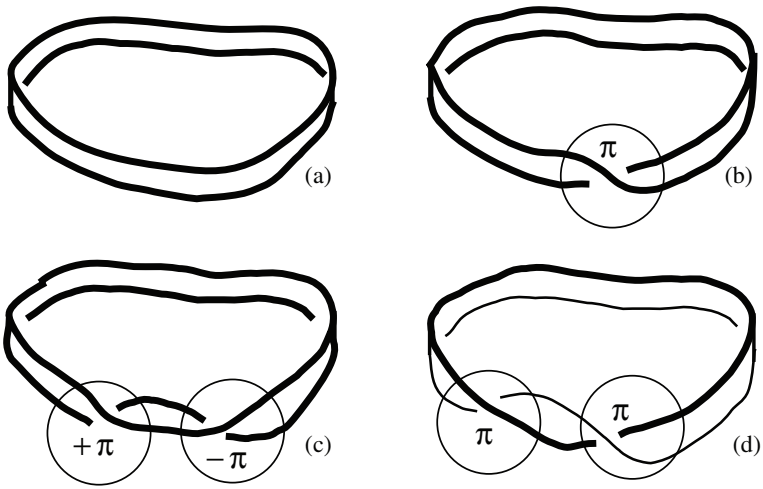

Figure 12.1. Topologically different rings of elastic strips: (a) nontwisted ring, $k = 0$; (b) Möbius strip, $k = 1/2$; (c) twisted strip with two identical edges, $k = 1$; (d) twisted strip with two distinctive edges, $k = 1$.

The allowed values of k are defined by the inner symmetry of the strip. For example, if the edges of the strip are different, e.g., marked by red and blue colors (Fig. 12.1.d), then only integer k's (2π-twists) are allowed.

Topological stability of twisted strips is similar to that of topological solitons; the issue of a singular core is not involved. Furthermore, one can draw a parallel between the twisted strips and singular defects. Imagine a circle around a π-disclination in a uniaxial nematic liquid crystal (Fig. 11.10). The set of molecules centered at this circle form a Möbius strip with $k = 1/2$. After going once around the circle, the director $\mathbf{n}$ flips into $-\mathbf{n}$, which is possible, because the nematic bulk is centrosymmetric, $\mathbf{n} \equiv -\mathbf{n}$. The number k would remain equal $1/2$ if the radius of the circle is taken larger or smaller (Fig. 11.10). Thus, the overall director configuration can be characterized by $k = 1/2$. At the disclination core, one faces the singularity: When the circle shrinks into a point, there is an infinity of director orientations at this point. If a disclination were created in a ferromagnet, a Möbius strip $k = 1/2$ around it would be impossible because the magnetization vector does not have the head-to-tail symmetry of the director.

To summarize, the examples above show that the topologically stable defects and configurations ("topological twists") obey the following general rules:

1. Defects types are related to the type of ordering of the system.
2. Defects are characterized by quantized invariants (topological charges) k.
3. The operations of merger and decay of the defects are described as certain operations (e.g., additions) applied to their charges k; conservation laws of topological charges control the results of merger and decay.

The topological invariants k's form groups. Because the concept of group is important for the homotopy classification of defects, we briefly consider it in the next sections. Before doing so, we briefly comment on, perhaps, the most intriguing twisted strips—the DNA molecules.

12.1.2. DNA and Twisted Strips, a Digression

Twisted strips with different k's are of relevance to the problem of configuration and replication of double-stranded DNA molecules. Two strands are arranged in a helicoid fashion in which a 2π-twist occurs per every 10.5 base pairs (Fig. 1.21). In many organisms ranging from viruses and prokaryotes to some eukaryotes, DNA molecules form closed loops. Topologically, these loops remind of a twisted strip with two distinctive edges and an integer Lk that is referred to as the *linking number* of the two strands (Fig. 12.2). Lk is preserved in any conformational change of DNA molecule that does not break the strands. If Lk is close to $Lk_0 = l/p$ (l is the total DNA length, and $p \approx 3.4$ is the helix pitch; Fig. 1.21), the DNA ring is relaxed and can lie flat on a planar surface without contortions. Often $Lk \neq Lk_0$: The ends of the relaxed linear DNA duplex may be additionally twisted (or untwisted) by some number of rotations $\pm 2\pi$ before forming the ring. There are two ways

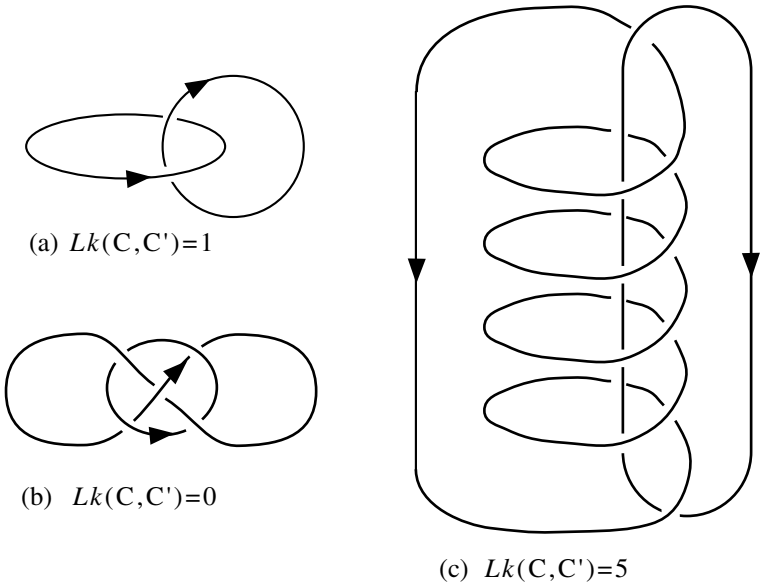

Figure 12.2. Linking numbers for pairs of oriented curves.

to deal with the induced strain. First, the number of base pairs per pitch can be changed; the ring remains *planar*, and the linking number is equal to the number of turns of one strand around another. In that case, $Lk = k$, the *topological* twist defined above. Second, the duplex axis can twist upon itself, leaving the number of pairs per pitch unaffected. Such a supertwisted DNA is no longer planar and coils in three dimensions, like a buckled twisted ribbon. Whatever the case, although k and Lk stay unaffected, and are still equal integral numbers of a *topological* nature, the global *geometry* (and consequently, the energy of the "twisted" ribbon and the way it relaxes) depends on the elasticity properties of the molecule and is better described by introducing two *geometrical* parameters: the *twist* Tw and the *writhe* Wr. The twist can be written as

$$Tw = \frac{1}{2\pi} \oint \Omega(s)\, ds, \tag{12.1}$$

where $\Omega(s)$ is the rate of wrapping of either strand about the duplex axis. This quantity can be defined equally for an open strip; Tw can take any value, and we can refer to it as the *geometrical* twist. However, if the duplex axis is planar, one gets $Lk = Tw = k$. The writhe Wr of a curve C is a much more subtle quantity. Introduced by Fuller, it is the number of averaged self-crossings (with sign) of the planar orthogonal projections of C (closed or not); in the DNA context, it describes the buckling of the duplex axis, so to speak. Like Tw,

Wr can take any value. We have the important relation:

$$Lk = Tw + Wr, \tag{12.2}$$

with *Lk* (for two oriented curves C and C′) and *Wr* (for an oriented curve C) given by double integrals:

$$Lk = \frac{1}{4\pi} \oiint_{C,C'} \frac{\mathbf{r}(\mathbf{s}) - \mathbf{r}(\mathbf{s}')}{|\,\mathbf{r}(\mathbf{s}) - \mathbf{r}(\mathbf{s}')\,|^3} \cdot [d\mathbf{s} \times d\mathbf{s}'];$$
$$Wr = \frac{1}{4\pi} \oiint_{C,C} \frac{\mathbf{r}(\mathbf{s}) - \mathbf{r}(\mathbf{s}^*)}{|\,\mathbf{r}(\mathbf{s}) - \mathbf{r}(\mathbf{s}^*)\,|^3} \cdot [d\mathbf{s} \times d\mathbf{s}^*]. \tag{12.3}$$

Here, C is the duplex axis, say, and C′ is anyone of the strands. *Wr* vanishes when C is planar. Note that for the example in Fig. 12.2 (b), $Lk(\mathrm{C}, \mathrm{C}') = 0$, because the two curves can be disentangled by crossing of a ∞-shaped line with itself; such crossings are not reflected in the integral *Lk* above.

To separate the DNA strands during replication, one needs to change the number *Lk* (see Problem 12.1). It can be done directly by topoisomerases that cut one or both strands. In other cases, the replication occurs through local binding of the DNA molecule to proteins that creates zones of negative and positive supertwisting.

12.1.3. Groups: Basic Definitions

Consider a set (finite or infinite, discrete or continuous) G of elements $a, b, c, \ldots$, for which there is an operation $\otimes$ that combines the elements in a prescribed way. The set G is a group if and only if the following requirements are satisfied:

1. Any two elements a, b in the set G can be combined by the operation $\otimes$ to produce a third element $a \otimes b$ in the set.
2. The operation is associative: $(a \otimes b) \otimes c = a \otimes (b \otimes c)$.
3. There is an identity element I of G, such that for any element a, $a \otimes I = I \otimes a = a$.
4. Every element a has an inverse element denoted a^{-1}, such that $a \otimes a^{-1} = a^{-1} \otimes a = I$.

A simple example of a group is a set Z of all integers with the operation of addition ($\otimes \to +$). Indeed, the axiom (2) is fulfilled when one adds integers; the identity element is 0; and the inverse to a is $-a$.

Groups are either commutative (also called Abelian) or noncommutative (or non-Abelian). For the Abelian groups, $a \otimes b = b \otimes a$ for any pair of elements. For non-Abelian groups, $a \otimes b \neq b \otimes a$. The group of integers is Abelian. Groups can contain a finite number of elements or infinitely many elements. Finite or denumerably infinite groups are called discrete groups. The additive group Z of integers is discrete.

A subgroup H of a group G is a subset of elements of G that is also a group. If h_i are the elements of the subgroup H and g is any element of G, then the set of elements-products $g \otimes h_i$ is called a *left coset* of H and the set $h_i \otimes g$ is called a *right coset* of H. It is easily proven that the cosets $g_1 \otimes h_i$ and $g_2 \otimes h_i$, formed by two elements g_1 and g_2 of G, are either identical or have no common elements whatever. In other words, a given subgroup H divides the group G into disjoint cosets that form a *coset space* or *orbit* denoted as G/H. The coset space is not necessarily a group. However, if the subgroup H is *normal* (also called *invariant*), meaning that the left and right cosets contain the same elements for each g of G, then the coset space G/H has a group structure and is called a *factor group*.

Two types of groups are important in the topological classification of defects of a given ordered medium, both related to the order parameter:

1. The (generally) continuous group G whose elements are in correspondence with all the permissible transformations of the order parameter. The group of symmetry H is a subgroup of this continuous group.
2. The discrete homotopy groups that are related to the topological structure of the order parameter space.

This will be detailed below. We first schematize how these groups are involved in the topological classification of defects.

12.1.4. General Scheme of the Topological Classification of Defects

Homotopy classification of defects in ordered media includes the following three steps:

First, one defines the order parameter (OP) ψ of the system. In a nonuniform state, the OP is a function of coordinates, $\psi(\mathbf{r})$.

Second, one determines the OP *(or degeneracy) space* $\mathcal{R}$, i.e., the manifold of all possible values of the OP that do not alter the thermodynamical potentials of the system. The function $\psi(\mathbf{r})$ maps the points of real space occupied by the medium, into $\mathcal{R}$.

The mappings of interest are those of i-dimensional spheres enclosing defects in real space. A point defect in a 2D system or a line defect in 3D can be enclosed by a linear contour, $i = 1$; a point defect in a 3D system can be enclosed by a sphere, $i = 2$; a wall defect can be "enclosed" by two points, $i = 0$, located at opposite sides of the wall.

Third, one defines the homotopy groups $\pi_i(\mathcal{R})$. The elements of these groups are mappings of i-dimensional spheres enclosing the defect in real space into the OP space. To classify the defects of dimensionality t' in a t-dimensional medium, one has to know the homotopy group $\pi_i(\mathcal{R})$ with $i = t - t' - 1$.

On the one hand, each element of the homotopy group corresponds to a class of topologically stable defects; all of these defects are equivalent to one another under continuous deformations. On the other hand, the elements of homotopy groups are topological in-

variants, or topological charges of the defects. The defect-free state (e.g., $\psi(\mathbf{r}) = \text{const}$) corresponds to a unit element of the homotopy group and to zero topological charge.

12.1.5. Order Parameter Space. Groups That Describe Transformations of the Order Parameter

The Heisenberg isotropic ferromagnetic phase with a unit magnetization vector $\mathbf{d}$ as the order parameter is an example of a medium for which the OP space is easily found by a qualitative consideration. This phase is isotropic in the sense that the coupling between $\mathbf{d}$ and the crystallographic axes is neglected. Any rotation about a fixed $\mathbf{d}$ transforms the system into itself. The ends of vectors $\mathbf{d}$ with different orientations in space describe a sphere S^2. Thus it is obvious that the OP space is the sphere S^2. For many other media, the situation is not that clear. Below, we illustrate a general way to find the OP space that sheds some light on the relationship between the symmetry of the ordered medium and the OP space.

Consider a continuous group of 3D rotations. This group is the part of the full Euclidian group of translations and rotations, which leaves the thermodynamic state of the system invariant. A 3D rotation can be specified by a vector $\mathbf{k}$ that is parallel to the axis of rotation and has an absolute value equal to the angle of rotation φ. Rotations around all possible axes having one common point form a group called *the group of proper rotations in 3D Euclidian space*. This group is represented by a solid 3D sphere of radius π denoted $SO(3)$ and composed of points $\varphi\mathbf{k}/|\,\mathbf{k}\,|$, where $-\pi \le \varphi \le \pi$. Two diametrically opposite points at the surface of such a sphere are identical: π-rotations around axes directed in opposite directions give the same result.

In principle, $SO(3)$ can serve as the OP space of the Heisenberg ferromagnet. However, there are sets of points in $SO(3)$ that correspond to *indistinguishable* stable states of the ferromagnet. Because any rotation around $\mathbf{d}$ transforms the system into itself, all points $\varphi\mathbf{d}$ along any fixed radius of the solid sphere $SO(3)$ describe indistinguishable states. Because of this symmetry, the solid sphere $SO(3)$ is "reduced" to the sphere S^2 by rotations that leave the order parameter $\mathbf{d}$ unchanged. The process is called a *factorization* of the group $SO(3)$ by the group $SO(2)$ of 2D rotations around the fixed axis $\mathbf{d}$ (Fig. 12.3). $SO(2)$ is a *subgroup* of $SO(3)$. The OP space of the ferromagnet is represented as $S^2 = SO(3)/SO(2)$, where $SO(3)/SO(2)$ is the notation for the *coset space* of $SO(2)$ in $SO(3)$. Note that S^2 is an example of a manifold. General definitions are given below.

If the medium is a uniaxial nematic, then the directions $\mathbf{d}$ and $-\mathbf{d}$ are identical and there is an additional factorization of S^2 by a set of two diametrically opposite points on S^2. The OP space of the uniaxial nematic is thus $\mathcal{R} = SO(3)/SO(2) \times Z_2 = S^2/Z_2$, also called the projective plane RP^2 (see Chapter 3). Z_2 is the group of two numbers 0 and 1: $0 + 0 = 1, 0 + 1 = 1, 1 + 0 = 1, 1 + 1 = 0$. The symbol $\times$ denotes a *direct product* of two groups $SO(2)$ and Z_2. The direct product of two groups, say, G and T, is

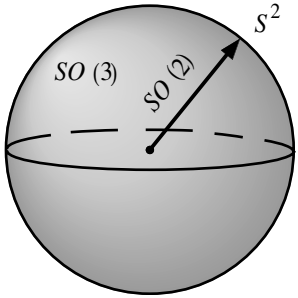

Figure 12.3. Factorization of the group $SO(3)$ of proper rotations by the group of rotations $SO(2)$ results in the sphere S^2.

the set $G \times T$ of pairs (g, t) that is a group under the combination law $(g_1, t_1) \otimes (g_2, t_2) = (g_1 \otimes g_2, t_1 \otimes t_2)$.

Examples above lead to the following generalization of the group-theoretical description of the OP space.

The order parameter of a continuous perfectly ordered medium can be associated with a "thermodynamic" group G (which is usually the Euclidian group) with elements g that transform a given value ψ_0 of the order parameter into another value $g\psi_0$ for which the thermodynamical potentials of the system remain the same. Rotations of a perfect ferromagnet as a whole are transformations of this kind. Among the elements g, there might be transformations that preserve not only the energy, but also the value of the order parameter, $g_H\psi_0 = \psi_0$. These elements form a subgroup H of G called the *isotropy group* of ψ_0 or the little group of ψ_0. The OP space is then the coset space $\mathcal{R}$, noted G/H:

$$\mathcal{R} = G/H. \tag{12.4}$$

Note that generally $\mathcal{R}$ is not a group. Furthermore, there is a certain arbitrariness in the choice of the group G (but not in $\mathcal{R}$!). The group G can be taken "larger" or "smaller," but the corresponding isotropy subgroup H must finally result in the same $\mathcal{R} = G/H$. If G is the full Euclidian group, then H is the group of symmetry of the ordered medium.

12.1.6. Homotopy Groups

Homotopy groups describe the topology of the OP space. Here, we briefly consider some abstract OP space $\mathcal{R}$ and the group of *oriented contours (loops)* in it that form the so-called *fundamental*, or *first homotopy group*.

Suppose that $\mathcal{R}$ is a connected surface: Any two points on $\mathcal{R}$ can be connected by a curve. Take an arbitrary point M that belongs to the surface and draw oriented continuous

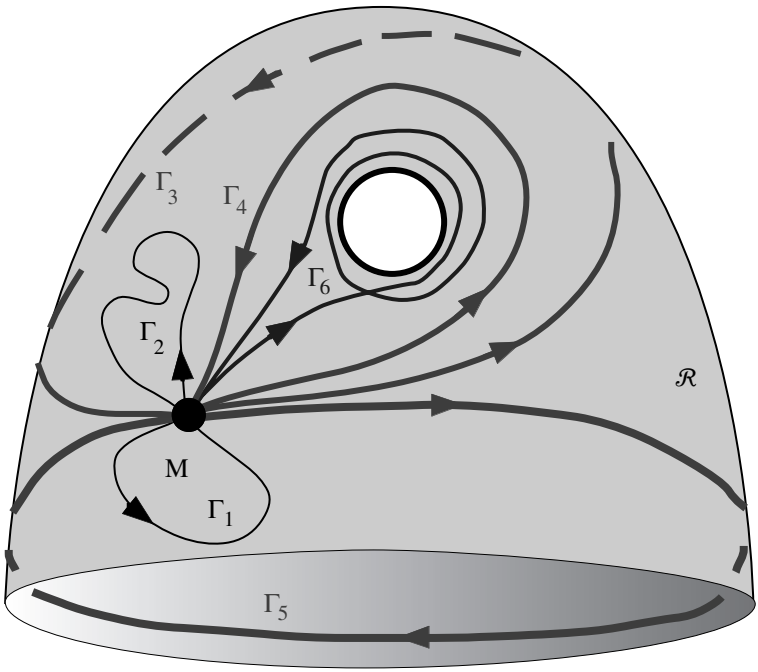

Figure 12.4. Oriented contours based at point M in the order parameter space $\mathcal{R}$. See text.

contours that start and end in M (Fig. 12.4). The contour is "oriented" when the direction of traversing is specified. Among the contours, there are some that can be continuously transformed into each other, such as contours Γ_1 and Γ_2 or Γ_3 and Γ_4 in Fig. 12.4. These contours are said to be *homotopic* or representing the same *homotopy class*. If $\mathcal{R}$ is connected (i.e., made of one piece only) and *simply connected* (no holes), then any contour can be contracted to a point M; thus, all the contours belong to the same homotopy class. If $\mathcal{R}$ is not simply connected (one example is a circle S^1, another is given by Fig. 12.4), then there are distinct classes of homotopic contours. For example, Γ_3 and Γ_5 in Fig. 12.4 that encircle different "holes," or Γ_4 and Γ_6 that encircle the same hole but a different number of times, belong to different homotopy classes. There is no continuous transformation between the contours from different homotopy classes.

One can introduce a product of two contours Γ_n and Γ_k as a contour Γ_{nk} obtained by first traversing Γ_n and then Γ_k: $\Gamma_{nk} = \Gamma_n \otimes \Gamma_k$. Figure 12.5 shows two homotopic representations of Γ_{nk}. Similarly to *the product of individual contours*, one can consider a *product of homotopy classes* as a set of products of representatives of these classes. This concept allows one to impose a group structure on the set of contours with the product of homotopy classes being the group operation. The elements of the group are the homotopic

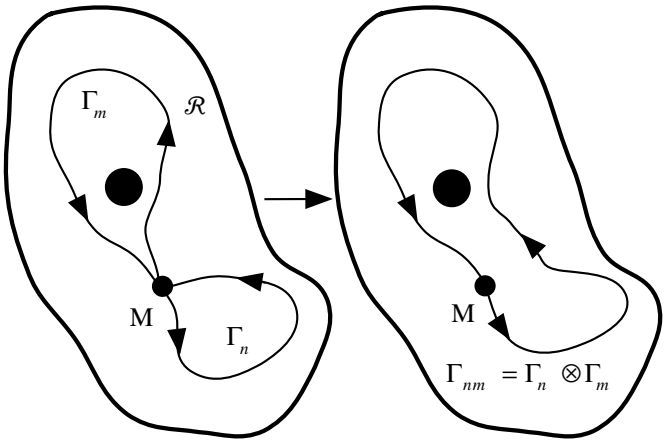

Figure 12.5. Two homotopic representations of Γ_{nk}, the contour product of the two contours Γ_n and Γ_k traversed in this order.

classes. The class of contours that are homotopic to zero (contractible to a single point) is the identity of the group. Each class has its inverse element that is the same set of contours but with opposite orientation. The product of classes satisfies the associative law. Thus, the set of homotopy classes of contours form a group called the *fundamental group of* $\mathcal{R}$ *at the base point* M and denoted $\pi_1(\mathcal{R}, \mathrm{M})$ or simply the *fundamental group of* $\mathcal{R}$, $\pi_1(\mathcal{R})$. This simplification in omitting the base point is possible when $\mathcal{R}$ is connected. If instead of M one chooses any other point M_1 in the connected space $\mathcal{R}$ as the base point, the resulting group $\pi_1(\mathcal{R}, \mathrm{M}_1)$ is an isomorphic copy of $\pi_1(\mathcal{R}, \mathrm{M})$. The group isomorphism is a one-to-one mapping of one group onto another that preserves the group operation. Thus, a connected OP space $\mathcal{R}$ can be characterized by a single abstract group $\pi_1(\mathcal{R})$. $\pi_1(\mathcal{R})$ is also called the first homotopy group to distinguish it from the nth homotopy groups $\pi_n(\mathcal{R})$ that are discussed later.

The fundamental group $\pi_1(\mathcal{R})$ can be Abelian or non-Abelian, depending on the OP space $\mathcal{R}$. If $\mathcal{R}$ is a 2D plane with one punched hole (homeomorphic to a circle S^1), then $\pi_1(\mathcal{R})$ is Abelian (Fig. 12.5). If $\mathcal{R}$ is a 2D plane with two punched holes (homeomorphic to the figure "8"), then the fundamental group is non-Abelian, $\Gamma_k \otimes \Gamma_n \neq \Gamma_n \otimes \Gamma_k$. As shown in Fig. 12.6, there is no way to pass continuously from $\Gamma_3 = \Gamma_1 \otimes \Gamma_2$ to $\Gamma_3^* = \Gamma_2 \otimes \Gamma_1$ with A a fixed point on Γ_3 and Γ_3^*.

This concludes the discussion of the OP space and homotopy groups needed to understand the general scheme of classification of topological defects. To illustrate the scheme, we first consider point defects in 2D nematic, smectic, and crystalline phases classified by the fundamental group. These examples require simple topological considerations. In the

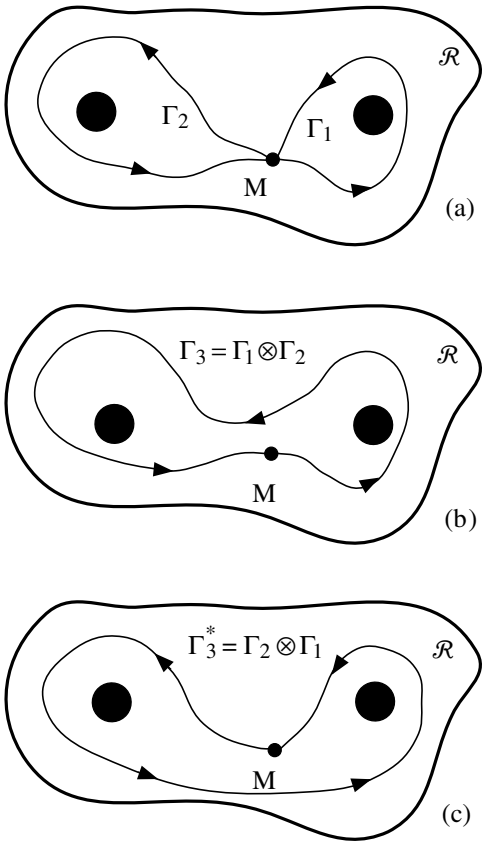

Figure 12.6. Contours in the order parameter space $\mathcal{R}$ (a plane with two punched holes). Base point M. $\Gamma_3 (= \Gamma_1 \otimes \Gamma_2) \neq \Gamma_3^* (= \Gamma_2 \otimes \Gamma_1)$ yield a non-Abelian fundamental group $\pi_1(\mathcal{R})$.

general case, more sophisticated group-theoretical methods are required to calculate the homotopy groups from the structure of G/H.

12.1.7. Point Defects in a Two-Dimensional Nematic Phase

In our model of a 2D nematic, the centers of gravity of molecules lie in one plane, while the director $\mathbf{n}$ makes the angle $0 \leq |\psi_0| \leq \pi/2$ with the normal $\boldsymbol{\nu}$ to the plane. The order parameter can be chosen either as a unit vector $\boldsymbol{\tau} = \mathbf{n} - \boldsymbol{\nu}(\mathbf{n} \cdot \boldsymbol{\nu})$ (which is a projection of $\mathbf{n}$ on the plane) or as the wave function $\psi = |\psi_0| \exp(i\varphi)$, where $|\psi_0|$ is the polar and φ is the azimuthal angle of the tilt of the molecules, respectively. The free energy density of

the uniform state does not depend on φ and can be represented as a certain function of the modulus $|\psi_0|$; e.g.,

$$F_{\text{cond}} = A|\psi|^2 + B|\psi|^4 \tag{12.5}$$

(cf. the description of superfluid helium; Section 3.1.1). The OP space $\mathcal{R}$ depends on the modulus $|\psi_0|$.

1. If $0 < |\psi_0| < \pi/2$, then $\mathcal{R} = S^1$. The phase φ can vary from 0 to 2π, and each point of S^1 corresponds to a certain value of φ. Fig. 12.7b shows the circle S^1 as the bottom of the free-energy density F_{cond} (see also Fig. 3.1).
2. If $|\psi_0| = \pi/2$, then $\mathcal{R} = S^1/Z_2$. Any two diametrically opposite points of the circle become identical, owing to the nonpolarity $\mathbf{n} \equiv -\mathbf{n}$ of the nematic. Topologically, S^1 and S^1/Z_2 are *identical*. However, there is an important physical difference between the defects at $0 < |\psi_0| < \pi/2$ and $|\psi_0| = \pi/2$, as we shall see below.
3. If $|\psi_0| = 0$, $\mathcal{R}$ is a single point.

Nonuniformity in the azimuthal orientation of molecules gives rise to an additional gradient energy term:

$$F_{\text{cond}} = A|\psi|^2 + B|\psi|^4 + \tfrac{1}{2}K|\nabla\psi|^2, \tag{12.6}$$

where K is the elastic constant of the in-plane splay and bend deformations. The energy density (12.6) determines a length scale that is called the coherence length $\xi = \sqrt{K/A}$. If the characteristic scale of distortions is much larger than ξ, the tilt angle is close to its equilibrium value $|\psi_{0,\text{eq}}| = \sqrt{-A/2B}$ and the inhomogeneity involves only the variations of the azimuthal angle $\varphi(x, y)$. This function $\varphi(x, y)$, or, equivalently, the function $\tau(x, y)$, maps the real 2D space (x, y) into $\mathcal{R}$. The study of mappings of closed contours around point defects in a 2D system enables one to determine whether the defects are stable.

As an example, let us elucidate the stability of three different points P_0, P_1, and P_2 in the $\boldsymbol{\tau}$ field for the case when $0 < |\psi_0| < \pi/2$, and thus, $\mathcal{R} = S^1$ (Fig. 12.7).

Let us surround the "suspicious" point by an oriented loop, such as γ_0 around point P_0. The mapping $\boldsymbol{\tau}(x, y)$ draws a corresponding oriented loop on S^1, such as Γ_0 in Fig. 12.7b. Γ_0 can be continuously contracted (without leaving the circle S^1) into a single point (Fig. 12.7d); accordingly, smooth rearrangement of the vector field $\boldsymbol{\tau}(x, y)$ in the real space results in a uniform state $\boldsymbol{\tau}(x, y) = \text{const}$ (Fig. 12.7c). The defect P_0 under test proved to be removable, or topologically unstable.

The situation differs for the radial-like configuration of $\boldsymbol{\tau}(x, y)$ (Fig. 12.7e). The loop Γ_1 runs around the entire circle S^1 and cannot be continuously contracted. To eliminate the defect in Fig. 12.7e, one has to destroy the condensed state along the entire line starting at P_1 (to cut Γ_1) or to allow appreciable deviation of the tilt angle from $|\psi_{0,\text{eq}}|$ (to separate Γ_1 from the circle S^1). Both cases require overcoming a considerable energy bar-

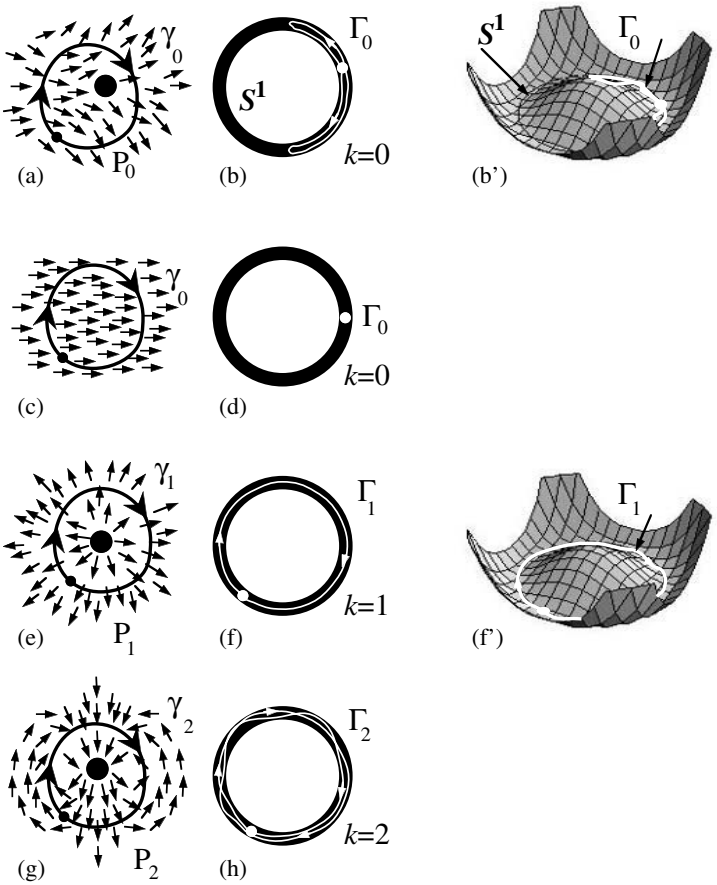

Figure 12.7. Point defects with different topological charges k in a polar 2D nematic with tilt angle $0 < |\psi_0| < \pi/2$; the arrows depict the projections of director on the plane: (a), (c) $k = 0$, defect-free state; (e) $k = 1$; g) $k = 2$; (b), (d), (f), (h) corresponding contours in the order parameter space S^1. (b') and (f') show S^1 as the circle of degenerate minima of the free energy potential; see text.

rier that greatly exceeds the energy of the in-plane distortions. In other words, the defect in Fig. 12.7e is topologically stable. The defect P_2 (Fig. 12.7g), whose contour Γ_2 runs twice around S^1, is also stable: It cannot be transformed into the uniform state nor into the radial-like defect.

The scheme above sets a correspondence between topologically stable defects and contours Γ_k that encircle S^1 k times in a given direction. All point singularities are divided into classes, each of which corresponds to its own class of homotopic contours Γ_k. The set of classes Γ_k forms the fundamental group $\pi_1(S^1)$. The definition of group is satisfied:

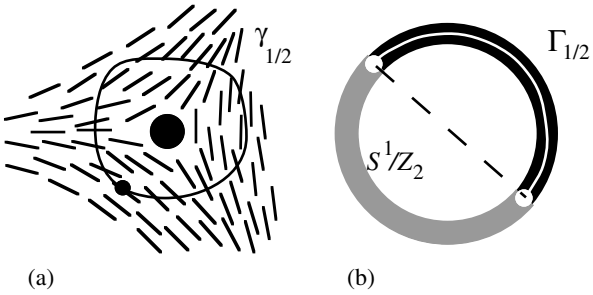

Figure 12.8. Defect $k = -1/2$ in a 2D, nonpolar nematic.

Any two contours Γ_k and Γ_n can be combined to give a third contour $\Gamma_{kn} = \Gamma_k \Gamma_n$ (we simplify the notations for product by dropping the symbol $\otimes$ from this point onward). The operation is associative; there is a special contour Γ_0 equivalent to a point, which is the identity element; contours Γ_k and Γ_{-k} that run around S^1 in opposite directions are the inverses of each other, $\Gamma_k \Gamma_{-k} = \Gamma_0$. Finally, $\pi_1(S^1)$ is Abelian.

Each element of $\pi_1(S^1)$ can be labeled by an integer k; thus, $\pi_1(S^1)$ is isomorphic to the group Z of integers. The number k is the topological charge of the defect. It cannot be changed by continuous deformations. Analytically, for point defects under consideration,

$$k = \frac{1}{2\pi} \oint_{\gamma} \nabla\varphi \, dl = 0, \pm 1, \pm 2, \ldots . \tag{12.7}$$

When $| \psi_0 | = \pi/2$, the degeneracy space is $\mathcal{R} = S^1/Z_2$, i.e., topologically identical to $\mathcal{R} = S^1/Z_2$. Thus, there are as many (infinitely many) defects in the case $| \psi_0 | = \pi/2$ as in the case $0 < | \psi_0 | < \pi/2$. However, physically, the two sets of defects are different: With $| \psi_0 | = \pi/2$, defects with an odd number of π-rotations are allowed and thus k can be integer or *half*-integer (Fig. 12.8a). In Fig. 12.8b, the contour $\Gamma_{1/2}$ that connects antipodal points of the circle is closed and cannot be contracted into a point; compare to Fig. 11.3d.

Finally, for $| \psi_0 | = 0$, there are no defects at all, and the fundamental group is trivial, $\pi_1(0) = 0$.

12.1.8. Point Dislocations in a Two-Dimensional Crystal

As was established in Chapter 3, the OP space of a 2D crystal is the direct product of two circles, i.e., the torus, $\mathcal{R} = S^1 \times S^1$ (we neglect the symmetries of rotation) (Fig. 3.7 and Fig. 12.9). Any in-plane displacement of a 2D crystal lattice as a whole leads just to another presentation of the crystal but does not change its thermodynamic potentials. If the displacement vector coincides with the primitive lattice vector, the transformation leads

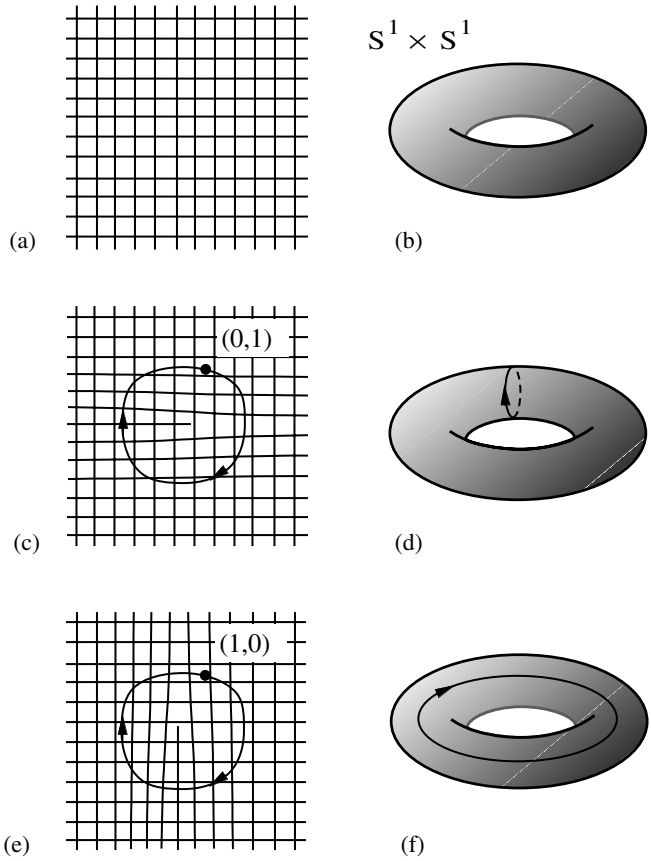

Figure 12.9. Point dislocations in a 2D crystal with the order parameter space $\mathcal{R} = S^1 \times S^1$.

to the identical state. The torus as the degeneracy space results from identification of the boundaries of a 2D Bravais cell.

The following basic types of loops cannot be contracted into a point on the torus: Those that run around the "small" circle (Fig. 12.9d), those that run around the "large" circle, (Fig. 12.9f), and their combinations. These loops correspond to point dislocations. Each dislocation is characterized by a pair of topological invariants (k_x, k_y) that shows how many times the loop runs about the "small" and the "large" circle, respectively:

$$\pi_1(S^1 \times S^1) = \pi_1(S^1) \times \pi_1(S^1) = Z \times Z = (k_x, k_y). \tag{12.8}$$

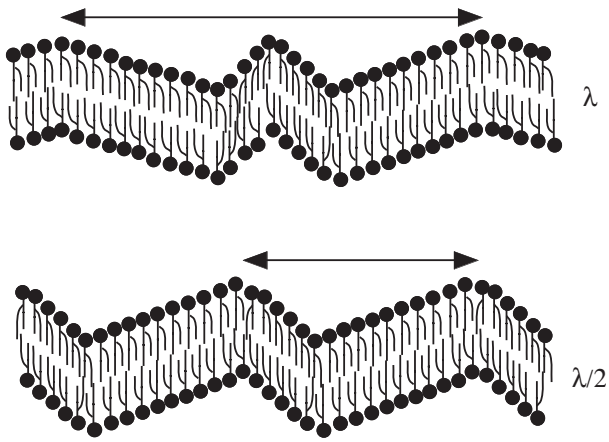

Figure 12.10. Molecular structure of the bilayers with λ- and λ/2-order in the $P_{\beta'}$ phase, shown in cross section by a plane normal to the bilayers. Arrows indicate the period of structures.

The numbers (k_x, k_y) in (12.8) are nothing else but the x and y-components of the Burgers vector $\mathbf{b}$ expressed in the units of the lattice repeat vectors $(\mathbf{a}_x, \mathbf{a}_y)$: $\mathbf{b} = k_x\mathbf{a}_x + k_y\mathbf{a}_y$.

A 2D smectic can be represented by a 2D medium with a 1D density wave. A close experimental model is the "rippled" lamellar lyotropic $P_{\beta'}$ phase composed of stacked lecithin bilayers with additional translational order along one of the two within-membrane directions. In-plane ordering makes the rippled membranes rigid; in principle, one can dilute the $P_{\beta'}$ phase and observe a behavior of a single bilayer in isolation. The bilayers of the $P_{\beta'}$ phase manifest two types of in-plane corrugated supermolecular structures—the λ-phase and the λ/2-phase (Fig. 12.10). The ridges and troughs of the membrane are equidistant and can be considered as a 2D smectic phase. The difference between the two is that the "layers" of the λ-phase are of equal width d, whereas in the λ/2-phase, the alternating odd and even "layers" are of different width; this asymmetric profile is observed for chiral surfactants.

To find the degeneracy space of the symmetric λ-phase, one has to consider both translation and rotation symmetries. A translation t by a multiple of d along the normal to the layers and a rotation r by an angle multiple of π bring the system into itself. The OP space is thus a rectangle $\{(t, r), 0 \le t \le d, 0 \le r \le \pi\}$ (Fig. 12.11a). A point (t, r) within the rectangle corresponds to a different representation of the 2D smectic; all of these representations have the same energy. The sides of the rectangle are identified by the rules $(0, r) \to (d, r)$ and $(t, 0) \to (d - t, \pi)$, as illustrated by the arrows in Fig. 12.11a. Note that after a rotation by π, a translation t transforms into $d - t$. This subtle point makes the resulting degeneracy space a Klein bottle (Fig. 12.11) rather than a torus. The fundamental group of the Klein bottle is non-Abelian and is isomorphic to a semidirect product of the

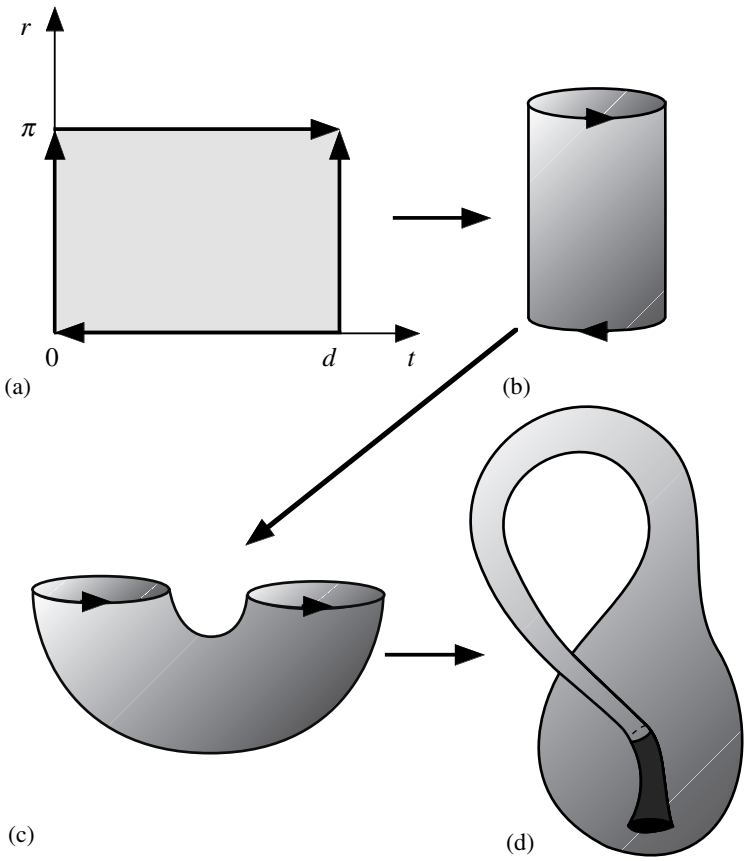

Figure 12.11. Equivalent presentations of the order parameter space of a 2D smectic: (a) a rectangle $\{(t, r), 0 \leq t \leq d, 0 \leq r \leq \pi\}$ with edges identified; (d) the same rectangle transformed into a Klein bottle through steps (b) and (c).

group Z_{tr} describing translations by the group Z_{rot} describing rotations, which are both isomorphic to Z:

$$\pi_1(\mathcal{R}_\lambda) = Z_{\text{tr}} \wedge Z_{\text{rot}}. \tag{12.9}$$

Consequently, every point defect in the λ-phase corresponds to a pair of numbers (n, m). Elements $(n, 0)$ correspond to point dislocations with Burgers vector $\mathbf{b} = nd$, and elements $(0, m)$ correspond to point disclinations of integer (even m's) and half-integer strength (odd m's). Here, the values of m are taken twice as large as those of the usual k's in order to better

represent the combinations of defects. The combination law for the semidirect product is different from that of a direct product. If n_1 and n_2 are two translations, and m_1 and m_2 are two rotations, then the combination law is $(n_1, m_1)(n_2, m_2) = (n_1 + m_1 n_2, m_1 + m_2)$.

Noncommutativity of the fundamental group $\pi_1(\mathcal{R}_\lambda)$ results in subtle physical effects. For example, the result of merger of two defects in the presence of a third defect is ambiguous and depends on the path of merger. In a non-Abelian medium, a point defect no longer corresponds to one element of the fundamental group, but to an entire class of *conjugated* elements. By definition, two elements a and b of a group G are said to be conjugate to one another if there is an element q of G such that $b = q^{-1}aq$. Figure 12.12 shows that a $(1, 0)$ dislocation after passing around a $(0, 1)$ disclination should be characterized by the pair $(-1, 0)$. In other words, the same defect is described by different elements $(1, 0)$ and $(-1, 0)$ that belong to the same conjugacy class. In the OP space, the contour $\Gamma_{(1,0)}$ transforms into the contour $\Gamma_{(-1,0)} = \Gamma^{-1}_{(0,1)}\Gamma_{(1,0)}\Gamma_{(0,1)}$ after the corresponding defect $(1, 0)$ goes around the $(0, 1)$ disclination. In an Abelian medium, $\Gamma_{(1,0)}$ and $\Gamma_{(0,1)}$ commute, and thus $\Gamma_{(1,0)}$ and $\Gamma_{(-1,0)}$ would be homotopic; however, in the noncommutative case, $\Gamma_{(1,0)}$ and $\Gamma_{(-1,0)}$ are not homotopic.

Because the same defect can correspond to different elements of the conjugacy class in a non-Abelian π_1, the coalescence of two defects is not uniquely defined. For example, a $(1, 0)$ dislocation and a $(-1, 0)$ "antidislocation" upon merging either annihilate (Fig. 12.13b) or form a double dislocation $(2, 0)$, if the point $(-1, 0)$ passed around the $(0, 1/2)$ disclination on the path to the merger site (Fig. 12.13c). The result is determined not by multiplication of individual elements of the homotopy group, as for Abelian media, but by all results of multiplication of classes of conjugated elements. Thus, to predict the result of merging, one has to know the global configuration of the order parameter; local topology around the defects is not enough.

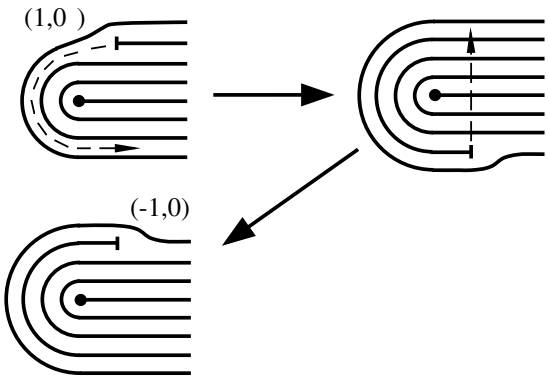

Figure 12.12. Conversion of a dislocation $(1, 0)$ into an antidislocation $(-1, 0)$ after circumnavigating around a disclination in the 2D smectic λ-phase.

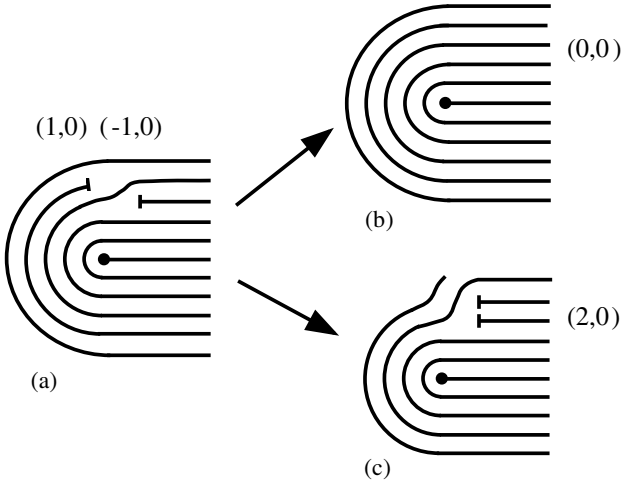

Figure 12.13. The result of merging of $(1, 0)$ and $(-1, 0)$ dislocations in the 2D smectic λ-phase depends on the path of merger around the disclination: (b) uniform state $(0, 0)$; (c) double dislocation $(2, 0)$.

The other variety of the $P_{\beta'}$ phase, the $\lambda/2$ structure, seemingly hardly differs from the λ structure (Fig. 12.10): Only the twofold symmetry axis C_2 has disappeared. However, now the order parameter space is a 2D torus T^2, and thus,

$$\pi_1(\mathcal{R}_{\lambda/2}) = Z_{\text{tr}} \times Z_{\text{rot}} \tag{12.10}$$

is a direct product of groups, and is commutative: The result of the merger of two defects is always unambiguous. Moreover, in contrast to the λ-phase, the $\lambda/2$-phase lacks isolated disclinations with an odd m.

Simple examples of λ- and $\lambda/2$-phases also reveal some restrictions of the homotopy theory for classifying defects in media with broken translational symmetry. According to the homotopy theory, (12.9) and (12.10), there might be disclinations with any integer m in a layered system. In reality, disclinations with m not equal to 1 or 2 ($k \neq 1/2, 1$) break the equidistance of layers and thus are energetically unfavorable.

12.2. The Fundamental Group of the Order Parameter Space. Line Defects

The fundamental group classifies topologically stable point defects in 2D-ordered media and topologically stable line defects in 3D.

12.2.1. Unstable Disclinations in a Three-Dimensional Isotropic Ferromagnetic

The OP space of the Heisenberg isotropic ferromagnet is a sphere S^2. Consider a disclination in the magnetization vector field. An oriented loop surrounding the disclination core in real space is mapped by the vector field into the OP space and, thus, produces a contour on S^2. Obviously, any contour drawn on a sphere can be contracted into a point. Thus, $\pi_1(S^2) = 0$: Any disclination in the 3D isotropic ferromagnet can be continuously transformed into a uniform state (Fig. 12.14).

The *topological* simplicity of the OP space should not let one believe that the question of defects in ferromagnets is trivial. There are interesting similarities between defects (points and lines) in nematics and ferromagnets, because the order parameters look very much alike, a vector in the case of a ferromagnet, a director in a nematic. But again the knowledge of nematic defects does not cover the knowledge of magnetic defects. The *physical* differences are indeed considerable. The subject of defects in ferromagnets will not be

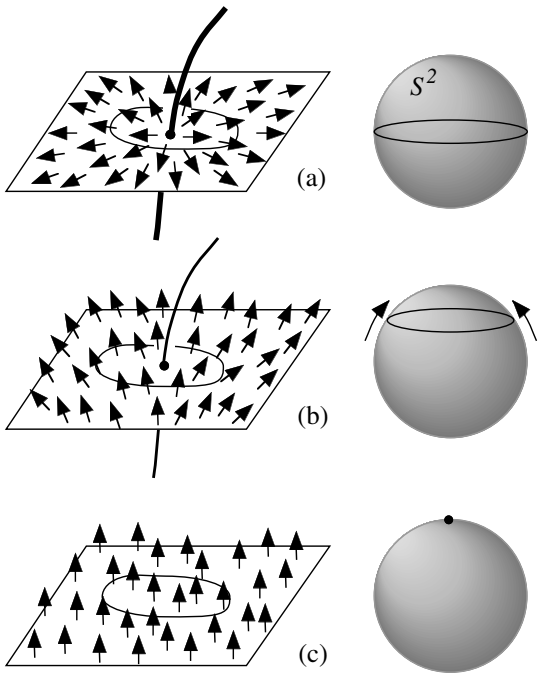

Figure 12.14. Continuous transformation of a disclination $k = 1$ (a) into a uniform state $k = 0$ (c) in a 3D ferromagnetic phase (left); corresponding contraction of a loop in the order parameter space (right).

pursued further. The interested reader might appreciate the specificity and the richness of this subject in the texts cited in "Further Reading."

12.2.2. Stable Disclinations in a Three-Dimensional Uniaxial Nematic Phase

In a 3D nonpolar uniaxial nematic phase, $\mathbf{n} \equiv -\mathbf{n}$, and the OP space is the sphere S^2/Z_2 or the projective plane RP_2.

There are two types of contours in S^2/Z_2: This is visible at once in the 2D representation of the projective plane (Fig. 3.6), where one notices contours that are actually closed (e.g., circles) and contours that are terminating at two diametrically opposite points. The first ones can shrink into a point; they correspond to disclinations of integer strength k that are topologically unstable. The second class of contours is not contractible to a point: under any continuous deformations, the ends of the contours remain fixed at the diametrically opposite points. These contours correspond to disclinations of half-integer k.

It is easy to see that all contours corresponding to half-integer k's can be transformed one into another (Fig. 12.15). Therefore, there is just one class of topologically stable

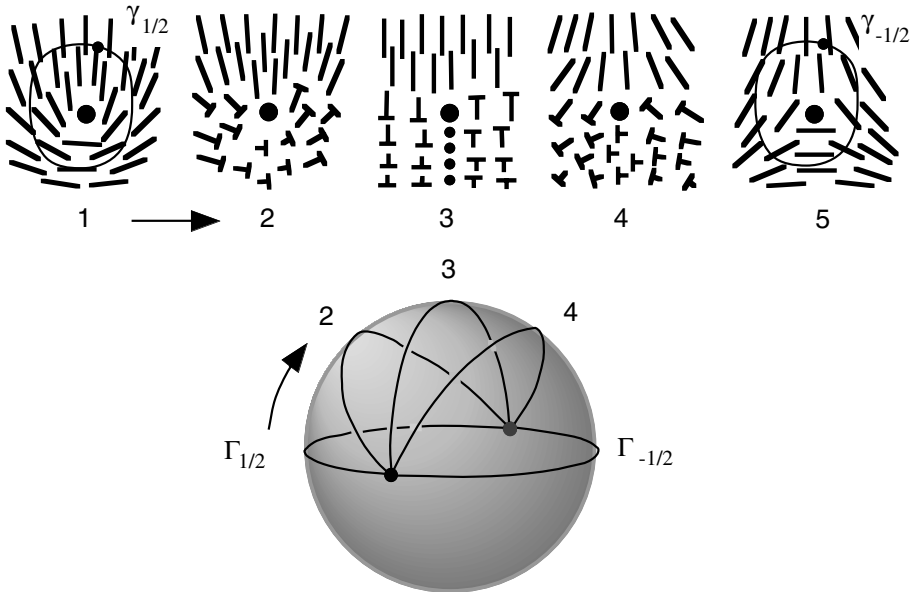

Figure 12.15. Continuous transformation of a disclination $k = 1/2$ into a disclination $k = -1/2$ in real space (director configurations above) and the corresponding transformation of contours in the OP space RP^2.

disclinations in the uniaxial nematic phase:

$$\pi_1(S^2/Z_2) = Z_2. \tag{12.11}$$

The laws of conservation are simply $1/2 + 0 = 1/2$ and $1/2 + 1/2 = 0$, if expressed in terms of k's.

12.2.3. Disclinations in Biaxial Nematic and Cholesteric Phases

Biaxial nematic order is specified by a tripod of mutually perpendicular directors $\mathbf{l} \equiv -\mathbf{l}$, $\mathbf{n} \equiv -\mathbf{n}$, and $[\mathbf{nl}] \equiv -[\mathbf{nl}]$. The OP space is the group $G = SO(3)$ of rotations of the triad $\mathbf{l}$, $\mathbf{n}$, $[\mathbf{nl}]$, factorized by the four-element point group D_2 of π-rotations about the directions $\mathbf{l}$, $\mathbf{n}$, and $[\mathbf{nl}]$:

$$R_{\text{bx}} = SO(3)/D_2. \tag{12.12}$$

Any two diametrically opposite points at the surface of $SO(3)$ are identical: π-rotations about axes oriented in opposite directions yield the same result, as discussed in Section 12.1.5. Thus, $SO(3)$ can be equivalently represented as the projective space $RP^3 = S^3/Z_2$ or as a 3D sphere in 4D space at which the antipodal points are identified, $SO(3) = S^3/Z_2$ (compare with the uniaxial nematic with OP space $RP^2 = S^2/Z_2$).

This is the place for some comments of general interest, which will be useful relating to media whose OP is a local triad (biaxial nematics, cholesterics). A standard method to calculate homotopy groups in the context of ordered media is *to lift* the topological space G to a *simply connected* space $\overline{G}$ (called the *universal cover* of space G), i.e., such that $\pi_1(\overline{G}) = 0$. In this process, any point $g \in G$ is lifted to a set of n (n independent of g) points g_i. Reciprocally, the *projection* on G of any $g_i \in \overline{G}$ and of a neighborhood V_i of g_i maps g_i and V_i on g and a neighborhood V of g. A path γ_{ij} on $\overline{G}$ from g_i to g_j maps on a closed loop Γ_{ij} in G, i.e., is in correspondence with one element of $\pi_1(G, g)$; i.e., n is the index of the fundamental group, or one of its subgroups (Massey). Note also that a subgroup $H \subset G$ lifts to a subgroup $\overline{H} \subset \overline{G}$, with relations of the type $g_i h_j = f_p$; $g_i, h_j, f_p \in \overline{G}$ if $gh = f$; $g, h, f \in G$. A simple ilustration of the properties above is with $G = S^1$, the 1D circle; its universal cover is a helix ($n = \infty$), which for simplicity, the reader can figure out as having the same radius as the circle, and staying "above" to visualize the projection process, although one must keep in mind that this "metrical" representation has no relation whatsoever with the topological properties that are considered here. Eventually, let us consider a subgroup $\overline{H} \subset \overline{G}$ that is the lift of a subgroup $H \subset G$. The fundamental group $\pi_1(G/H) = \pi_1(\overline{G}/\overline{H})$, because the coset spaces are the same, $\mathcal{R} = G/H = \overline{G}/\overline{H}$. Now, consider the manifold obtained by identifying any point $\overline{g}$ in $\overline{G}$ with all points $\overline{h}^{-1}\overline{g}\overline{h}$; $\overline{h} \in \overline{H}$ belonging to the subgroup conjugated to $\overline{g} \in \overline{G}$. Clearly, this manifold represents $\mathcal{R}$. Furthermore, $\pi_1(\overline{G}/\overline{H}) = \overline{H}$, because $\overline{G}$ is simply connected; a complete demonstration requires more sophisticated methods than those possible in the frame of this textbook.

The universal cover of the projective plane is the sphere S^2; similarly, the universal cover of $SO(3)$ is S^3. In both cases, $n = 2$. Consider $\overline{G} = S^3$; the symmetry group of the triad of directors is D_2, an Abelian subgroup of $SO(3)$ with four elements, which we shall denote I, i, j, and p, with the relations $i^2 = I, ij = ji = p$, where I is the identity and each other element is a π rotation about one of three different perpendicular axes. The lift of D_2 into S^3 is a group with eight elements. We call these elements, as the above, I, i, j, and p, adding the supplementary elements J, $-i$, $-j$, and $-p$, whose notations mean that they are, one by one, on the same "fibers" lifted over $SO(3)$ (therefore, their geometrical interpretation is the same). This is enough to obtain the new group relations, remembering the remark of the latter paragraph (viz. $g_i h_j = f_p$; $g_i, h_j, f_p \in \overline{G}$ if $gh = f$; $g, h, f \in G$). This eight-element group, noted Q, is non-Abelian and obeys the multiplication rules:

$$\begin{aligned} &ij = -ji = p, \quad jp = -pj = i, \quad pi = -ip = j, \\ &JJ = I, \quad ii = jj = pp = J, \quad ijp = J. \end{aligned} \tag{12.13}$$

It is the group of quaternion units. Eventually, one finds

$$\pi_1(S^3/D_2) = Q \tag{12.14}$$

The elements of the quaternion group form five conjugacy classes $C_0 = \{I\}, \overline{C}_0 = \{J\}$, $C_x = \{i, -i\}$, $C_y = \{j, -j\}$, and $C_z = \{p, -p\}$.

Disclinations in biaxial nematics differ sharply from disclinations in uniaxial nematics. Among them, one should distinguish five, rather than one, classes of topologically stable lines, which correlate with the five classes of conjugated elements of the group Q. Correspondingly, the topological charge can acquire the values I, J, $(i, -i)$, $(j, -j)$, $(p, -p)$, with the multiplication rules (12.13). Different disclinations are shown in Fig. 12.16. The strength k can be half-integer (π rotation of a director around the core, classes C_x, C_y, and

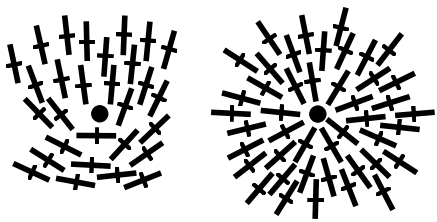

(a) (b)

Figure 12.16. Director fields **n** (long rods) and **l** (short rods) for topologically stable disclinations in a biaxial nematic: (a) $k = 1/2$, class C_z; (b) $k = 1$, class $\overline{C}_0$. Cross sections in a plane perpendicular to the axes of the disclinations are shown.

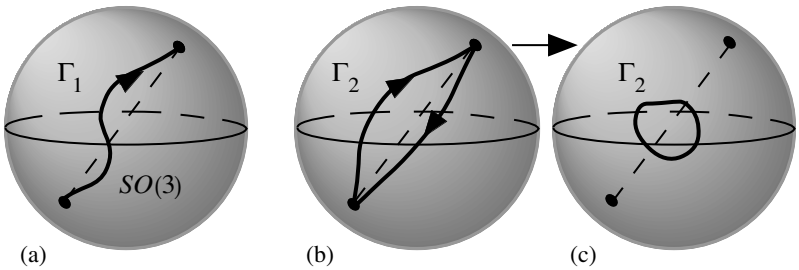

Figure 12.17. Closed contours Γ_1 (a) and Γ_2 (b), (c) corresponding to $|k| = 1$ and $|k| = 2$ disclinations in the OP space of the biaxial nematic. Both contours connect diametrically opposite and equivalent points at the surface of $SO(3)$. Γ_1 cannot continuously shrink into a point. Γ_2 runs between the two antipodal points twice (b) and can smoothly leave these points and shrink into a point (c).

C_z) or integer (2π-rotation, class $\overline{C}_0$). The singular core of the 2π disclination *cannot* be eliminated by the "escape in third dimension" as in the uniaxial nematic (Figs. 12.16 and 12.17). In contrast, 4π-disclinations, class C_0, $|k| = 2$, are topologically unstable. The striking difference between a 2π- and a 4π-lines is illustrated in Fig. 12.17.

The merger and decay of disclinations in the biaxial nematic obey the multiplication rules that are specific to the classes of elements, rather than the elements themselves. The results are given in Table 12.1.

If two disclinations belonging to two different classes merge, then a disclination is formed that belongs to the class of the product of the first two. The result of merger of disclinations of the same class from the set C_x, C_y, C_z is ambiguous: Either a nonsingular trivial configuration (class C_0) or a disclination from class $\overline{C}_0$ can be formed, depending on the path of merger with respect to other defect lines in the system.

The cited features of the disclinations merger stem from the noncommutativity of the group Q. Another spectacular consequence shows up in the entanglement of disclinations in biaxial nematics.

Table 12.1. Multiplication rules of five classes of elements of the quaternion group that control the merger and decay of disclinations in a biaxial nematic.

	C_0	$\overline{C}_0$	C_x	C_y	C_z
C_0	C_0	$\overline{C}_0$	C_x	C_y	C_z
$\overline{C}_0$	$\overline{C}_0$	C_0	C_x	C_y	C_z
C_x	C_x	C_x	C_0 or $\overline{C}_0$	C_z	C_y
C_y	C_y	C_y	C_z	C_0 or $\overline{C}_0$	C_x
C_z	C_z	C_z	C_y	C_x	C_0 or $\overline{C}_0$

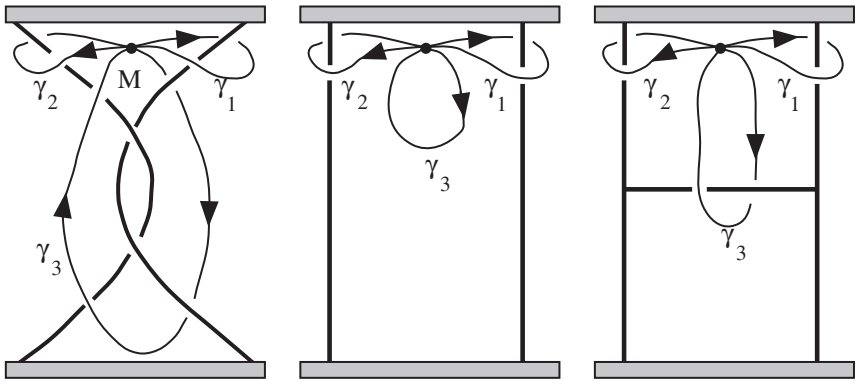

Figure 12.18. (a) Entanglement of disclinations in a biaxial nematic; (b) topologically trivial; (c) nontrivial.

Figure 12.18a shows two entangled disclinations. The question is whether they can be transformed by continuous variations of the directors into an unlinked configuration (Fig. 12.18b), if we require that the ends of the disclinations remain fixed.

To find the answer, let us draw three contours γ_1, γ_2, and γ_3 from a point M of real space: γ_1 and γ_2 encircle the defect lines, and γ_3 encircles the entangled region (Fig. 12.18). Their images in OP space will be some contours Γ_1, Γ_2, and Γ_3. Evidently, the defects can be unlinked only when Γ_3 is homotopic to zero. If this is not so, then separation of the disclinations will leave a topologically nontrivial trace in space, a third disclination (Fig. 12.18c). The result depends on the nature of the linked disclinations. One can show (Fig. 12.19) that the contour Γ_3 is homotopic to the product $\Gamma_1\Gamma_2\Gamma_1^{-1}\Gamma_2^{-1}$; an element of this form is called a *commutator* in the fundamental homotopy group. For Abelian groups, the commutator is the identity element, because $\Gamma_1\Gamma_2 = \Gamma_2\Gamma_1$. This is not true for non-Abelian groups; in particular, for the group Q, the contour Γ_3 can belong either to the class $C_0(\Gamma_1\Gamma_2\Gamma_1^{-1}\Gamma_2^{-1} = 1)$ or to the class $\overline{C}_0(\Gamma_1\Gamma_2\Gamma_1^{-1}\Gamma_2^{-1} = -1)$. The latter situation occurs when the two entangled disclinations belong to different classes from the set C_x, C_y, C_z. Therefore, after drawing two different disclinations $|k| = 1/2$ through one another, they prove to be connected by a disclination $|k| = 1$ belonging to $\overline{C}_0$.

The topological classification of defects in biaxial nematics can be applied to cholesterics, when the cholesteric pitch is much smaller than is the characteristic scale of deformations, as discussed in Chapter 11, where for convenience, we used the same notations for the classes of disclinations. However, the topological classification considered above does not apply, in its full generality, to the coarse-grained picture of cholesterics that takes into account the high energy cost of changing the cholesteric pitch.

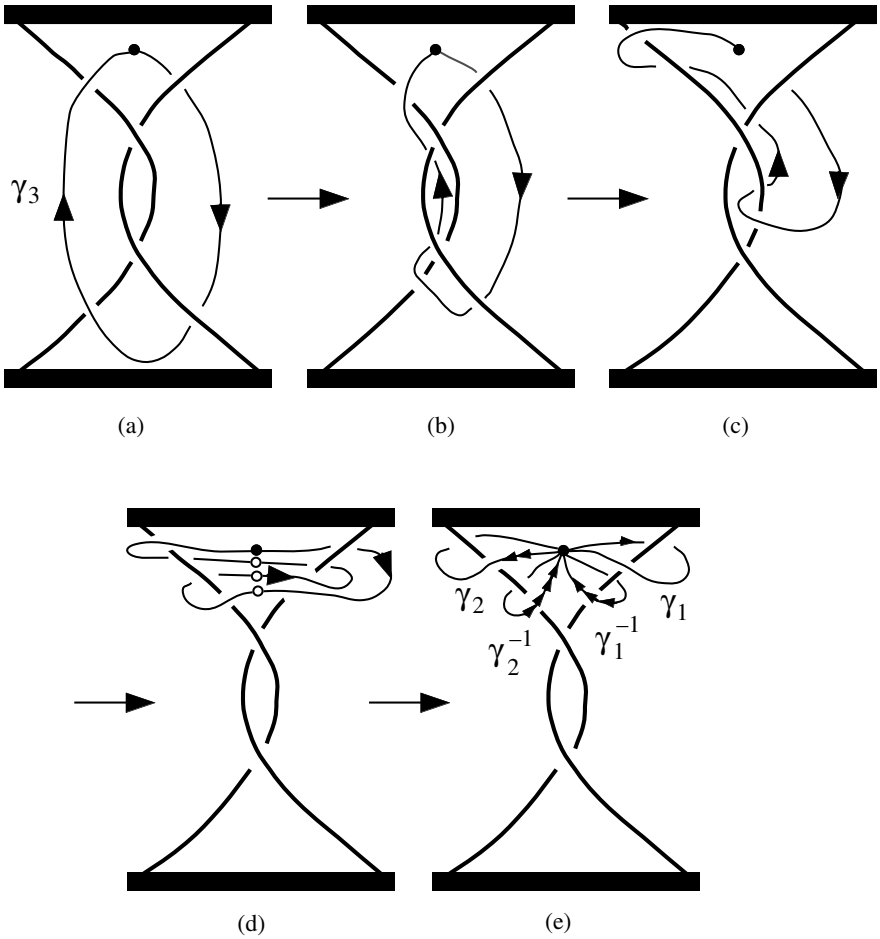

Figure 12.19. Continuous deformations of the contour γ_3 from Fig. 12.18 into the product contour $\gamma_1\gamma_2\gamma_1^{-1}\gamma_2^{-1}$, demonstrating that the image Γ_3 of γ_3 in OP space is homotopic to the product $\Gamma_1\Gamma_2\Gamma_1^{-1}\Gamma_2^{-1}$. At the step (d), one pinches together four points marked by circles.

12.3. The Second Homotopy Group of the Order Parameter Space and Point Defects

Point defects in 3D ordered phases are classified by the elements of the second homotopy group.

12.3.1. Point Defects in a Three-Dimensional Ferromagnet

In a 3D isotropic ferromagnet, the magnetization field $\mathbf{m}(\mathbf{r})$ may contain singular points at which the direction of $\mathbf{m}$ is not specified. To elucidate the topological stability of such a point, one encloses it with a closed surface σ (Fig. 12.20).

The radius of the sphere should be much larger than the core size of the point defect. The function $\mathbf{m}(\mathbf{r})$ produces a mapping of the surface σ into some surface in the OP space $\mathcal{R} = S^2$ (Fig. 12.20). If the resulting surface Σ can be contracted to a single point (Fig. 12.20a), the point defect is topologically unstable. If Σ is wrapped $N \neq 0$ times around the sphere S^2, the point singularity is a stable defect with topological charge

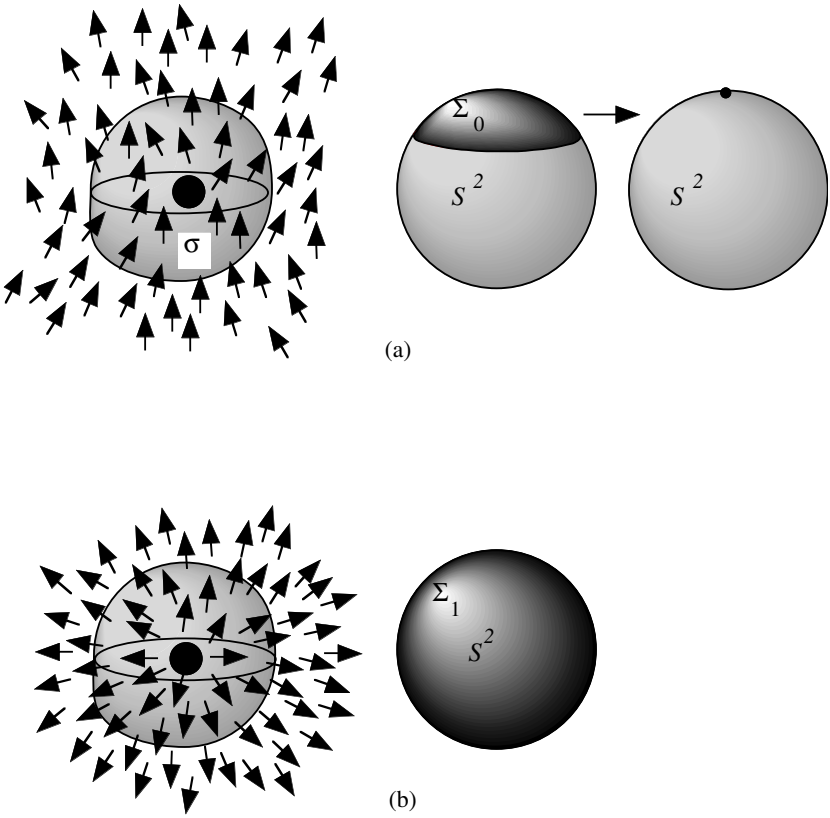

Figure 12.20. Topological stability of a point defect in a ferromagnet, core region (black ball) surrounded by a closed surface σ. (a) Unstable point defect; (b) topologically stable point defect.

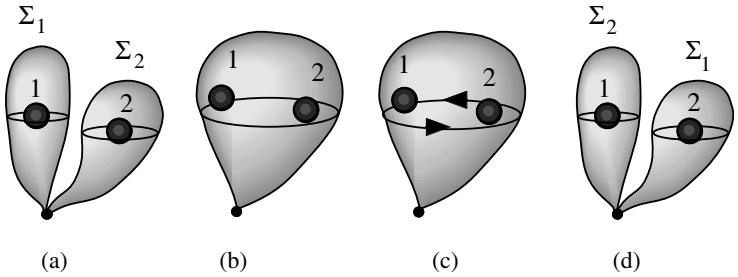

Figure 12.21. Multiplication of classes of surfaces, e.g., Σ_1 and Σ_2, is a commutative operation: $\Sigma_1\Sigma_2 = \Sigma_2\Sigma_1$. The arrow in (c) shows deformation of rotation. Redrawn from Mineev.

$N \neq 0$. For example, Fig. 12.20b illustrates a "hedgehog" radial defect, $\mathbf{m}(\mathbf{r}) = \mathbf{r}/|\,\mathbf{r}\,|$, for which Σ covers the entire sphere S^2 once, $N = 1$. The classes of all images Σ's (including the surfaces homotopic to a single point) form the *second homotopy group* $\pi_2(S^2)$, which in the case of the ferromagnet is isomorphic to the group of integers Z. The topological charge N of a point defect is also called the degree of mapping of σ on S^2. N shows how many times the vector $\mathbf{m}$ runs over the sphere S^2 in moving over the closed surface σ. In the example above, $\mathbf{m}(\mathbf{r}) = \mathbf{r}/|\,\mathbf{r}\,|$, and $N = 1$; if one reverses the orientation of $\mathbf{m}$, i.e., $\mathbf{m}(\mathbf{r}) = -\mathbf{r}/|\,\mathbf{r}\,|$, then the degree of mapping also changes the sign: $N = -1$. When the point defects coalesce, the charges N add up.

In contrast to $\pi_1(\mathcal{R})$, groups $\pi_2(\mathcal{R})$ are always Abelian; i.e., the multiplication of classes of surfaces Σ is commutative. Figure 12.21 shows a continuous deformation that establishes $\Sigma_1\Sigma_2 = \Sigma_2\Sigma_1$.

12.3.2. Topological Charges of Point Defects

Analytically, the topological charge of a point defect in a 3D unit vector field $\mathbf{m}$ is defined as an integral[1] over the sphere σ:

$$N^{(3)} = \frac{1}{4\pi}\int\limits_{\sigma} \mathbf{m}\cdot\left[\frac{\partial\mathbf{m}}{\partial u_1}\times\frac{\partial\mathbf{m}}{\partial u_2}\right] du_1\, du_2. \tag{12.15a}$$

The integrand contains the Jacobian of the transformation from the coordinates u_1 and u_2 on the sphere σ to the vector components $\mathbf{m}$ parameterizing the surface Σ that covers the OP S^2-sphere N times. If the vector field is parameterized as $\{n_x; n_y; n_z\} = \{\sin\theta\cos\varphi; \sin\theta\sin\varphi; \cos\theta\}$, with both angles θ and φ being the functions of the two

[1] M. Kleman, Phil. Mag. **27**, 1057 (1973); N.D. Mermin and T.-L. Ho, Phys. Rev. Lett. **36**, 594 (1976).

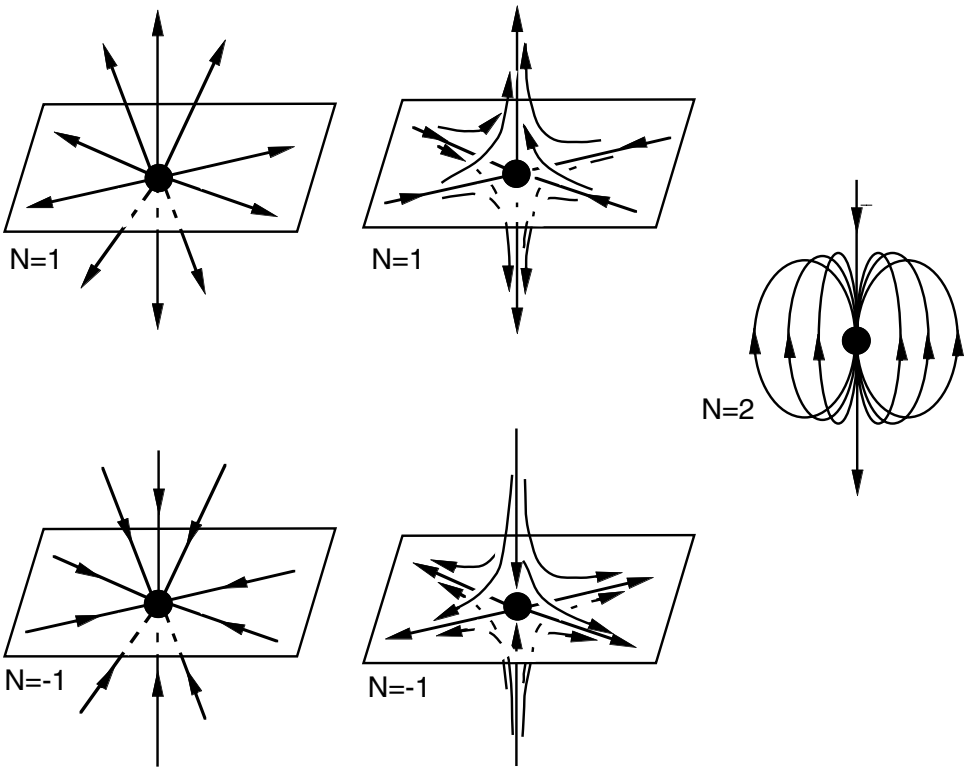

Figure 12.22. Point defects in a 3D vector field.

angular spherical coordinates u_1 and u_2, then

$$N^{(3)} = \frac{1}{4\pi} \int_0^{2\pi} du_2 \int_0^{\pi} \left(\frac{\partial\theta}{\partial u_1} \frac{\partial\varphi}{\partial u_2} - \frac{\partial\theta}{\partial u_2} \frac{\partial\varphi}{\partial u_1} \right) \sin\theta \, du_1. \tag{12.15b}$$

For a radial hedgehog, $N^{(3)} = 1$, as expected. Different 3D point defects are shown in Fig. 12.22.

In a similar way, one can define the topological charge of a 2D unit vector field $\boldsymbol{\tau}$ with components $\tau^1(l)$ and $\tau^2(l)$ as the integral over the coordinate l on a contour around the defect [compare with (11.4)]:

$$N^{(2)} = \frac{1}{2\pi} \oint \left(\tau^1 \frac{d\tau^2}{dl} - \tau^2 \frac{d\tau^1}{dl} \right) dl \quad (= 0, \pm 1, \pm 2, \ldots.) \tag{12.16}$$

Note that the two 2D radial configurations: "sink" ($\boldsymbol{\tau}$ directed toward the core) and "source" ($\boldsymbol{\tau}$ directed outward from the core), have the same invariant $N^{(2)} = 1$, in contrast to the 3D radial configurations, in which a reversal in the direction of $\mathbf{m}$ changes the sign of $N^{(3)}$.

12.3.3. Point Defects in a Three-Dimensional Nematic Phase

Classification of point defects in a 3D uniaxial nematic, $\mathcal{R} = S^2/Z_2$, is similar to that in a ferromagnet: $\pi_2(S^2/Z_2) = Z$. However, because $\mathbf{n} \equiv -\mathbf{n}$, each point can be equally assigned a charge N and a charge $-N$ (12.15). This ambiguity in the sign of the topological charge is the consequence of nontriviality of the fundamental group $\pi_1(S^2/Z_2)$ and its action on the group $\pi_2(S^2/Z_2)$.

Assume that the nematic volume contains a point defect and a π-disclination line. The director field provides a mapping of degree N of the sphere σ enclosing the point defect and part of the line defect, on S^2/Z_2. A point $\mathbf{r}_0$ of real space is mapped into an image point $\mathbf{n}(\mathbf{r}_0)$ of OP space. If one moves the point $\mathbf{r}_0$ over a closed contour γ around the disclination line, then the point $\mathbf{n}(\mathbf{r}_0)$ goes over a contour $\Gamma_{1/2}$ into an antipodal point $-\mathbf{n}(\mathbf{r}_0)$ and N reverses sign (Fig. 12.23). The contour $\Gamma_{1/2}$ connecting $\mathbf{n}(\mathbf{r}_0)$ and $-\mathbf{n}(\mathbf{r}_0)$ is a nontrivial element of the group $\pi_1(S^2/Z_2) = Z_2$. If the contour $\Gamma_{1/2}$ were the identity element, the degree of mapping would preserve the sign.

Thus, when $\pi_1(\mathcal{R})$ is nontrivial, each point singularity corresponds to a few elements (such as N *and* $-N$ above) of $\pi_2(\mathcal{R})$, rather than to a single element of $\pi_2(\mathcal{R})$ (such as N *or* $-N$). These elements are tranformed one into another by moving the image points along contours that are nontrivial elements of $\pi_1(\mathcal{R})$. The coalescence of two point defects N_1 and N_2 in the presence of disclination can result in a defect with a charge $|N_1 + N_2|$

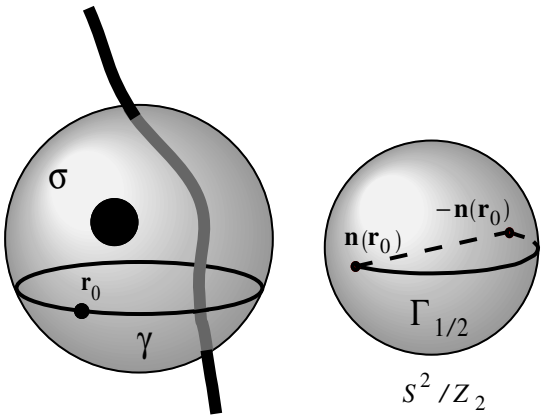

Figure 12.23. Action of the fundamental group π_1 on the second homotopy group π_2 in a uniaxial nematic: Moving point $\mathbf{r}_0$ of real space around a π-disclination transforms the image point $\mathbf{n}(\mathbf{r}_0)$ into an antipodal point $-\mathbf{n}(\mathbf{r}_0)$.

or $|N_1 - N_2|$, depending on the path of coalescence. Owing to this feature, all hedgehogs in a nematic system with a π-disclination can be annihilated, or at least all but one with $N = 1$ (if the total charge is odd).

12.4. Solitons

12.4.1. Planar Solitons

Let us study a uniaxial nematic placed in a plane capillary, both surfaces of which impose planar achoring in one direction **h**. The director in the bulk is set to be oriented along **h**: $\mathbf{n} = \pm\mathbf{h}$. In other words, the interaction with the walls contracts the OP space of the nematic to a single point. Let a vertical disclination $k = \pm 1/2$ exist in the specimen. When the disclination is present, it is impossible to conserve a uniform configuration $\mathbf{n} = \pm\mathbf{h}$: at a certain surface supported by the disclination, the director will undergo a π-rotation (Fig. 12.24a). The width of the wall is fixed by the balance of elastic and surface anchoring

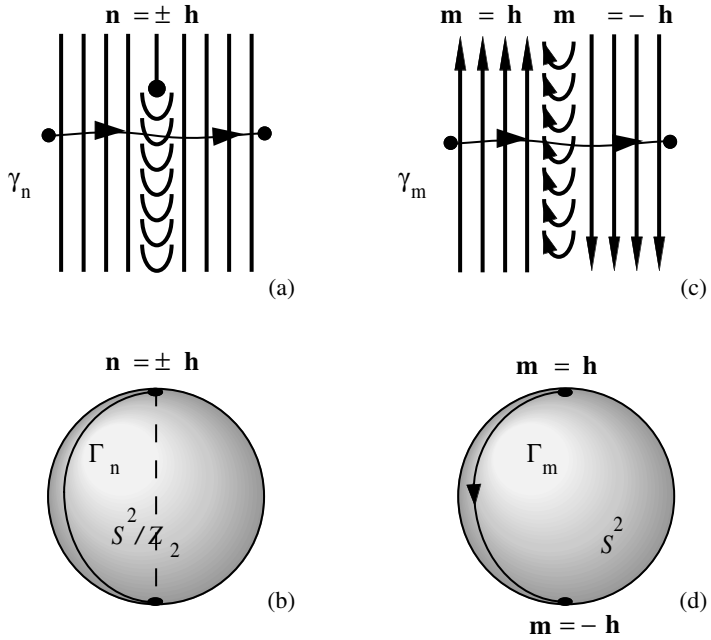

Figure 12.24. (a), (b) Topologically stable planar soliton in a uniaxial nematic; (c), (d) Bloch domain wall in an anisotropic ferromagnetic with an "easy magnetization" axis.

energies. If we write the energy of the wall as

$$F = \frac{Kd}{\rho} + w\rho, \tag{12.17}$$

then its equilibrium width ρ_0 is

$$\rho_0 = \left(\frac{Kd}{w}\right)^{1/2}. \tag{12.18}$$

Here, d is the thickness of the capillary, K is a nematic elastic constant, and w (dimension $\mathrm{J/m^2}$) is the anchoring coefficient, calculated as the energy per unit surface area needed to deviate the director from the "easy axis" $\mathbf{n} = \pm\mathbf{h}$ by the angle $\pi/2$. Such walls with a nonsingular director configuration are called planar solitons of topological type.

Not only does the soliton under consideration preserve a constant width, but it also possesses a nontrivial topological charge. Indeed, let us study the mapping of the line γ_n threaded through the soliton into the OP space (Fig. 12.24a). The ends of the line are mapped into antipodal identical points $\mathbf{n} = \pm\mathbf{h}$, whereas the line γ_n is mapped onto the closed contour Γ_n, linking these points on S^2/Z_2 (Fig. 12.24). This contour cannot be contracted to a point by any continuous transformations, which determines the topological stability of the planar soliton.

In the general case, the classes of homotopic mappings of the line γ threaded through a planar soliton form the *relative homotopy* group $\pi_1(\mathcal{R}, \overline{\mathcal{R}})$, where $\overline{\mathcal{R}}$ is the region of possible values of the order parameter far from the core of the soliton, narrowed in comparison to $\mathcal{R}$ by additional interaction (external field, boundary conditions, etc.). If $\overline{\mathcal{R}}$ consists of a single point, as in the case being studied, the group $\pi_1(\mathcal{R}, \overline{\mathcal{R}})$ coincides with the fundamental group $\pi_1(\mathcal{R})$. Therefore, soliton walls in nematics exist in a mutually one-to-one correspondence with the disclinations that have produced them and are described by the same group $\pi_1(S^2/Z_2) = Z_2$. If $\overline{\mathcal{R}}$ is not a point, then to find $\pi_1(\mathcal{R}, \overline{\mathcal{R}})$, one first finds $\pi_1(\mathcal{R})$ and then excludes from $\pi_1(\mathcal{R})$ the elements that correspond to $\pi_1(\overline{\mathcal{R}})$. In other words, one must find the factor group of $\pi_1(\mathcal{R})$ by its subgroup, which is the image of the homomorphism $\pi(\overline{\mathcal{R}}) \to \pi(\mathcal{R})$:

$$\pi_1(\mathcal{R}, \overline{\mathcal{R}}) = \pi_1(\mathcal{R})/\mathrm{Im}\left[\pi_1(\overline{\mathcal{R}}) \to \pi_1(\mathcal{R})\right]. \tag{12.19}$$

There are other examples of walls, different from the planar solitons above, that occur in media with disconnected $\overline{\mathcal{R}}$ (Fig. 12.24c). For example, consider a ferromagnet in which additional interaction between the magnetization vector and the crystal lattice is anisotropic. In equilibrium, the vector $\mathbf{m}$ orients along a particular crystallographic axis, say, $\mathbf{m} = \pm\mathbf{h}$. The states $\mathbf{m} = \mathbf{h}$ and $\mathbf{m} = -\mathbf{h}$ are distinguishable, unlike in the nematic

phase. Thus, $\mathcal{R}$ is reduced from the sphere S^2 into a set of two disconnected points $\mathbf{m} = \pm\mathbf{h}$ (Fig. 12.24d). The set of disconnected pieces of OP space $\mathcal{R}$ is denoted $\pi_0(\mathcal{R})$. In our case, $\pi_0(\mathbf{m} = \pm\mathbf{h}) = Z_2$ and any two domain walls can be merged to produce a uniform state. Alternatively, one can use the relative fundamental group $\pi_1(\mathcal{R}, \overline{\mathcal{R}}) = \pi_1(S^2, \mathbf{m} = \pm\mathbf{h})$; however, with a disconnected $\overline{\mathcal{R}}$, $\pi_1(\mathcal{R}, \overline{\mathcal{R}})$ is no longer a group. Domain walls of the type of the Bloch and Néel walls that provide a connection between different pieces of the disconnected OP space can be called "classical domain walls" to distinguish them from soliton walls ending at linear defects. This terminological distinction has a physical basis: To remove a wall associated with a linear singularity, it suffices to create a ring of disclinations in the plane of the wall. The latter, in expanding, "eats up" the wall; at the same time, to remove a classic wall requires overcoming a considerably larger energy barrier and transformation of the order parameter over the entire half-space on one side of the wall.

12.4.2. Linear Solitons

Just as a disclination in an external field can give rise to a planar soliton, a point defect can give rise to a linear soliton (Fig. 12.25). Linear solitons are described by the classes of mapping of the surface σ crossing the soliton into the OP spaces $\mathcal{R}$ and $\overline{\mathcal{R}}$, i.e., by the elements of the relative group $\pi_2(\mathcal{R}, \overline{\mathcal{R}})$. If a uniaxial nematic is oriented by a magnetic field $\mathbf{B}$ along the axis $\mathbf{h}||\mathbf{B}$, then $\overline{\mathcal{R}_N}$ reduces to one point, and $\pi_2(\mathcal{R}_N, \overline{\mathcal{R}_N}) = \pi_2(\mathcal{R}_N) = \pi_2(S^2/Z_2) = Z$; i.e., the classification of linear solitons coincides with the classification of hedgehogs.

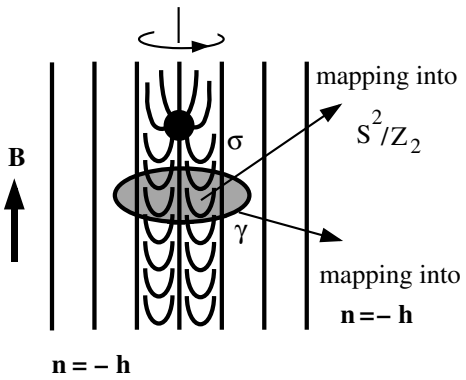

Figure 12.25. Linear soliton terminating at a point defect (a radial hedgehog in a nematic liquid crystal). The magnetic field $\mathbf{B}$ is along the axis $\pm\mathbf{h}$. See text.

12.4.3. Particle-Like Solitons

The distribution of the order parameter in particle-like solitons depends on all three coordinates. They are described by the group $\pi_3(\mathcal{R}, \overline{\mathcal{R}})$ of homotopy classes of the mappings of the 3D spherical volume D^3 containing the soliton into the space $\mathcal{R}$. Here, the boundary of the spherical volume, the sphere σ, is mapped into the narrowed space $\overline{\mathcal{R}}$. If $\overline{\mathcal{R}}$ consists of one point, then the particle-like soliton is described by the group $\pi_3(\mathcal{R})$. The spherical volume D^3 with all point of its surface σ being equivalent, is homotopic to a 3D sphere S^3 in a 4D space. Thus, the elements of $\pi_3(\mathcal{R})$ are mappings $S^3 \to \mathcal{R}$. Special cases $S^3 \to S^2$ and $S^3 \to S^2/Z_2$ are called Hopf mappings and correspond to $\pi_3(S^2) = \pi_3(S^2/Z_2) = Z$ (Fig. 12.26).

In a uniaxial nematic, the particle-like soliton amounts to a director configuration distorted in a region of finite size, outside of which the director field is uniform. As a rule, such solitons are unstable with respect to decrease in size and subsequent disappearance on scales smaller than the coherence length ξ. The decrease in size $L \to \mu L(\mu < 1)$ entails an increase in the elastic-energy density by a factor of $1/\mu^2$ and a decrease in the soliton's volume by a factor of μ^3, so that the total elastic energy decreases: $F \to F\mu$. Stabilization of particle-like solitons can be facilitated by an additional interaction, in particular, by helical twisting of the structure. In a weakly twisted cholesteric mixture, Bouligand observed two linked disclination rings $k_1 = k_2 = 1$, each of which by itself is topologically

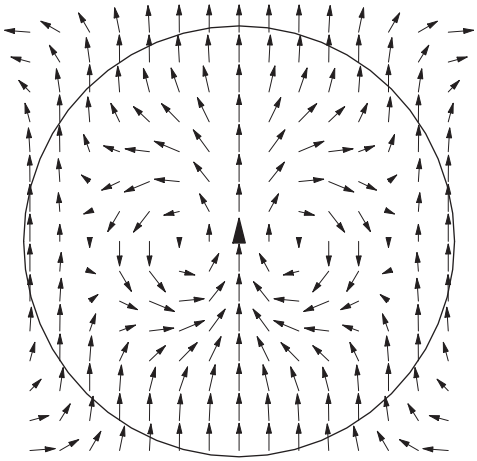

Figure 12.26. A nontrivial Hopf texture in a 3D vector field, as seen in the vertical cross section. The vector field is directed north everywhere outside of the sphere and at the origin. The vertical axis is the rotational symmetry axis. When going along any radius from the center to the surface of the sphere, the vector rotates by an angle $2\pi r/R$ around this radius. The length of the arrows is proportional to the length of vector projection in the XY plane.

unstable, whereby all points of the cores of the disclination are mapped into a single point of the degeneracy space S^2/Z_2. In going from one ring to the other, the director undergoes a 180° rotation, and one can represent the rings as inverse images of two diametrically opposite points on the sphere S^2. Evidently, one cannot convert the configuration into a homogeneous state because the rings are linked: Upon trying to unlink the rings, they must intersect one another and singularities would arise in the configuration. The degree of linking of the rings, equal in this case to unity, coincides with the Hopf invariant, which is an element of the group $\pi_3(S^2/Z_2) = Z$. The stability of the configuration as a whole is guaranteed by the conservation of the Hopf invariant.

Problem 12.1. Prepare a paper strip with a 2π-twist. Mark the edges of the strip in different colors. Imagine that the strip models a simple loop of a duplex DNA molecule. The DNA must be duplicated every time a cell divides. The two strands of the initial DNA must separate, and then each should synthesize its new partner to form a double-stranded DNA. Try to prepare the paper strip for a "replication" by cutting it along the central line; in a real DNA, it would correspond to the cutting of the hydrogen bonds between the base pairs. Repeat the cutting along the central line two times. Describe the topology of the result at each step. Compare the behavior of 2π-, π-, and untwisted strips.

Hint. The exercise should demonstrate the need in topoisomerases invented by Nature to change topology of the duplex DNA by cutting one or two of its strands.

Problem 12.2. The linking number *Lk* of two curves is an integer (12.3) that does not change when the curves are deformed without crossing each other. Calculate the linking number for the pair of circles $x^2 + y^2 = 1$ and $(y-1)^2 + z^2 = 1$.

Answers: $Lk = 1$. Parameterize the circle $x^2 + y^2 = 1$ as

$$\mathbf{r}_{c'}(\mathbf{s}') = (\cos \mathbf{s}', \sin \mathbf{s}', 0),\ 0 \le \mathbf{s}' \le 2\pi;$$

enlarge the circle $(y-1)^2 + z^2 = 1$ (without crossing the first circle) so that it can be parameterized as $\mathbf{r}_c(\mathbf{s}) = (0, 0, s)$, $-\infty < s < \infty$. According to (12.3),

$$Lk = \frac{1}{4\pi} \int_{-\infty}^{\infty} \int_{0}^{2\pi} \frac{ds ds'}{(1+s^2)^{3/2}} = \frac{1}{2} \int_{-\infty}^{\infty} \frac{ds}{(1+s^2)^{3/2}} = 1.$$

Problem 12.3. Let G be a group of transformations g that transform a given value of the order parameter ψ into another value $g\psi$ for which the thermodynamical potentials of the system remain the same. Let H be a set of all transformations g_H that leave the order parameter unchanged, $g_H \psi = \psi$. Prove that H is a subgroup of G.

Answers: If g_{H_1} and g_{H_2} leave the OP unchanged, so does $g_{H_1} g_{H_2}^{-1}$.

Problem 12.4. Find the OP spaces and fundamental groups of the 3D smectic A and smectic C [M. Kleman and L. Michel, J. Phys. Lett. **39**, L-29 (1978)].

Answers: In view of the complexity of the OP spaces of SmA and SmC phases, the direct algebraic approach to calculations is difficult. One can use an intuitive graphic scheme.

The density function of SmA and SmC is modulated along the normal to the layers with a period d_0 of the order of the molecular length (or larger, as in some diluted lyotropic lamellar phases). Within the layers, the density is constant, and the molecules are either normal to the layers (SmA) or tilted (SmC). The orientational order of both SmA and SmC, just like a nematic phase, is described by the director **n**. Taking into account also the translational order, the OP space for the SmA phase can be written as a filled torus $\mathcal{R}_A = (S^2/Z_2)\times S^1$. The vertical cross sections of the torus in the form of two circles amount to hemispheres S^2/Z_2 stretched into disks whose points characterize the orientation of **n**. The points along the large circles of the torus correspond to points along the segment $[0, d_0]$ closed into a circle S^1. At $(S^2/Z_2) \times S^1$, there are two types of elementary contours not homotopic to zero: the ones that join diametrically opposite points of the disks S^2/Z_2 (describing disclinations) and the ones that run around the hole of the torus (describing dislocations). The fundamental group $\pi_1(\mathcal{R}_A) = \pi_1(S^1)\times\pi_1(S^2/Z_2) = Z \times Z_2$ is composed of elements (b, k), where b is an integer and k is either 0 or 1/2. Combinations of dislocations and disclinations with both b and k being nontrivial are called *disgyrations*.

For the SmC phase, the order parameter can be easily represented by using the relationship $\mathcal{R}_A = \mathcal{R}_C/S^1$, which implies that each point of $\mathcal{R}_A$ corresponds in $\mathcal{R}_C$ to an entire family S^1 of points that specify the orientation of the tilted molecules in the plane of the SmC layers. Direct calculations show that $\pi_1(\mathcal{R}_C) = Z \wedge Z_4$, where $Z_4 = (I, a, a^2, a^3)$ is the group of subtractions modulo 4 with the unit element I.

Problem 12.5. A nonbounded biaxial nematic contains a π-disclination C_x and a 2π-disclination $\overline{C}_0$. Find the way to eliminate the disclination $\overline{C}_0$.

Hint. Split the $\overline{C}_0$-disclination into two (which ones?) and bring them together (along which paths?).

Problem 12.6. Find the relative homotopy group $\pi_1(\mathcal{R}, \overline{\mathcal{R}})$ when $\mathcal{R}$ is a torus $S^1 \times S^1$ and $\overline{\mathcal{R}} = S^1$.

Answers: $\mathrm{Im}\,[\pi_1(\overline{\mathcal{R}}) \to \pi_1(\mathcal{R})] = \pi(\overline{\mathcal{R}}) = Z$, $\pi_1(\mathcal{R}, \overline{\mathcal{R}}) = Z \times Z/Z = Z$ [V.P. Mineyev and G.E. Volovik, Phys. Rev. B **18**, 3197 (1978)].

Problem 12.7. Calculate the topological charge of the following vector fields in 2D:

(a) $(x, -y)/\sqrt{x^2 + y^2}$;

(b) $(-x, -y)/\sqrt{x^2 + y^2}$;

(c) $(x^2 - y^2, 2xy)/(x^2 + y^2)$;

(d) $(x^2 - y^2, -2xy)/(x^2 + y^2)$;

(e) $(x^3 - 3xy^2, -y^3 + 3x^2y)/(x^2 + y^2)^{3/2}$.

Hints. Parameterize the vector field using the coordinate $0 \le l \le 2\pi$ at the circle $(\cos l, \sin l)$. For example, the field (e) adopts the form $(\cos 3l, \sin 3l)$.

Answers: (a) -1; (b) 1; (c) 2; (d) -2; (e) 3.

Problem 12.8. Calculate the topological charges and the elastic energy of the following two hedgehogs in the nematic bulk of radius R:

$$\mathbf{n}_1 = (x, y, z)/\sqrt{x^2 + y^2 + z^2} \quad \text{and} \quad \mathbf{n}_2 = (-x, -y, z)/\sqrt{x^2 + y^2 + z^2}.$$

Use the Frank–Oseen free energy density with elastic constants

$$K_1 \neq K_2 \neq K_3 \neq K_{24}, K_{13} = 0.$$

Answer: See (11.14) in Chapter 11.

Further Reading

General Courses

M. Kleman, Points, Lines, and Walls in Liquid Crystals, Magnetic Systems, and Various Ordered Media, John Wiley & Sons, Chichester, 1983.

T. Frankel, The Geometry of Physics: An Introduction, Cambridge University Press, 1997.

D.J. Thouless, Topological Quantum Numbers in Nonrelativistic Physics, World Scientific, Singapore, 1998.

Knots and Strips

Louis H. Kauffman, Knots and Physics, 3rd Edition, World Scientific, Singapore 2001.

W. F. Polh, J. Math. Mech. **17**, 975 (1968).

J. H. White, Am. J. Math. **91**, 693 (1969).

F. B. Fuller, Proc. Nat. Acad. Sci. USA **68**, 815 (1981).

DNA Topology and Its Biological Effects, Edited by N. Cozzarelli and J.C. Wang, Cold Spring Harbor Laboratory Press, 1990.

Geometry and Algebraic Topology

D. Hilbert and S. Cohn-Vossen, Geometry and the Imagination, Chelsea Publishing, New York, 1952.

N. Steenrod, Topology of Fiber Bundles, Princeton University Press, 1951.

W. S. Massey, Algebraic Topology: An Introduction, Harcourt, Brace & World, Inc., New York, 1967.

Reviews of Homotopy Theory Applied to Defects in Ordered Media

N.D. Mermin, Rev. Mod. Phys. **51**, 591 (1979).

L. Michel, Rev. Mod. Phys. **52**, 617 (1980).

V.P. Mineev, Sov. Sci. Rev. Sect. A, Vol. 2, Edited by I.M. Khalatnikov, Chur, London, Harwood Academic, New York, 1980.

H.-R. Trebin, Adv. Phys. **31**, 194 (1982).

Topological Stability

G. Toulouse and M. Kleman, J. Phys. Lett. (Paris) **37**, L-149 (1976); M. Kleman, J. Phys. Lett. (Paris) **38**, L-199 (1977).

G.E. Volovik and V.P. Mineev, Pis'ma Zh. Eksp. Teor. Fiz. **24**, 605 (1976) [JETP Lett. **24**, 595 (1976)]; Zh. Eksp. Teor. Fiz. **72**, 2256 (1977) [Sov. Phys. JEPT **46**, 1186 (1977)].

Y. Bouligand, Physics of Defects, Edited by R. Balian, M. Kleman, and J.-P. Poirier, North-Holland, Amsterdam, 1981, p. 665.

M. Kleman and L. Michel, Phys. Rev. Lett. **40**, 1387 (1978).

Y. Bouligand, B. Derrida, V. Poénaru, Y. Pomeau, and G. Toulouse, J. Phys. (Paris) **39**, 863 (1978).

Comparison with Experiments in Liquid Crystals

M.V. Kurik and O.D. Lavrentovich, Usp. Fiz. Nauk **154**, 381 (1988)/Sov. Phys. Usp. **31**, 196 (1988).

Biaxial Nematics

G. Toulouse, J. Phys. Lett. (Paris) **38**, L-67 (1977).

Defects in Anisotropic Superfluids

G.E. Volovik, Exotic Properties of Superfluid 3He, World Scientific, Singapore, 1992.

Defects in Ferromagnets

M. Kleman, Dislocations, disclinations, and magnetism, in "Dislocations in Solids," 5, Edited by F.R.N. Nabarro, North-Holland, Amsterdam,1980.

M. Kleman, Magnetization processes in ferromagnets, in "Magnetism of Metals and Alloys," Edited by M. Cyrot, North-Holland, Amstredam, 1980.

A. P. Malozemoff and J. C. Slonczewski, Magnetic Domain Walls in Bubble Materials, Academic Press, New York, 1979.